

1. Title Page

Drug-drug interaction between metformin and sorafenib alters antitumor effect in hepatocellular carcinoma cells

Rania Harati^{1,2}, Marc Vandamme², Benoit Blanchet^{3,4}, Christophe Bardin³, Françoise Praz^{2,5}, Rifat Akram Hamoudi^{6,7}, Christèle Desbois-Mouthon^{2,8}

¹ *Department of Pharmacy Practice and Pharmacotherapeutics, College of Pharmacy, University of Sharjah, Sharjah, United Arab Emirates*

² *Centre de Recherche Saint-Antoine, Sorbonne Université, INSERM, F-750012 Paris, France*

³ *Département de Pharmacocinétique et Pharmacochimie, Hôpital Cochin, AP-HP, CARPEM, F-75014 Paris, France*

⁴ *UMR8038 CNRS, U1268 INSERM, Faculté de Pharmacie, Université de Paris, PRES Sorbonne Paris Cité, F-75006 Paris, France*

⁵ *Centre National de la Recherche Scientifique, Paris, France*

⁶ *Department of Clinical Sciences, College of Medicine, University of Sharjah, Sharjah, United Arab Emirates*

⁷ *Division of Surgery and Interventional Science, UCL, London, United Kingdom*

⁸ *Centre de Recherche des Cordeliers, Sorbonne Université, INSERM, Université de Paris, F-75006 Paris, France*

2. Running title Page

Running title: Metformin and sorafenib in hepatocellular carcinoma

Corresponding author : Christèle Desbois-Mouthon, PhD
Centre de Recherche des Cordeliers
INSERM UMR_S1138
15 rue de l'école de médecine
75006 Paris
France
e-mail: christele.desbois-mouthon@inserm.fr

Number of pages: 51

Number of tables: 2

Number of figures: 6

Number of references: 61

Number of words in abstract: 207

Number of words in introduction: 594

Number of words in discussion: 1351

List of abbreviations: ADAM8: ADAM metallopeptidase domain 8; AMPK: AMP-activated protein kinase; CCL20: C-C motif chemokine ligand 20; CEACAM1: carcinoembryonic antigen-related cell adhesion molecule 1; FGF2: fibroblast growth factor 2; GPCR: G-proteins coupled receptor; HCC, hepatocellular carcinoma; MASH: metabolic-associated steatohepatitis; MAPK: mitogen-activated protein kinase; MTT: 3-(4,5-dimethylthiazol-2-yl)-2,5-diphenyltetrazolium bromide; OATP, organic anion-transporting polypeptide; RTK, receptor tyrosine kinase; T2D: type 2 diabetes.

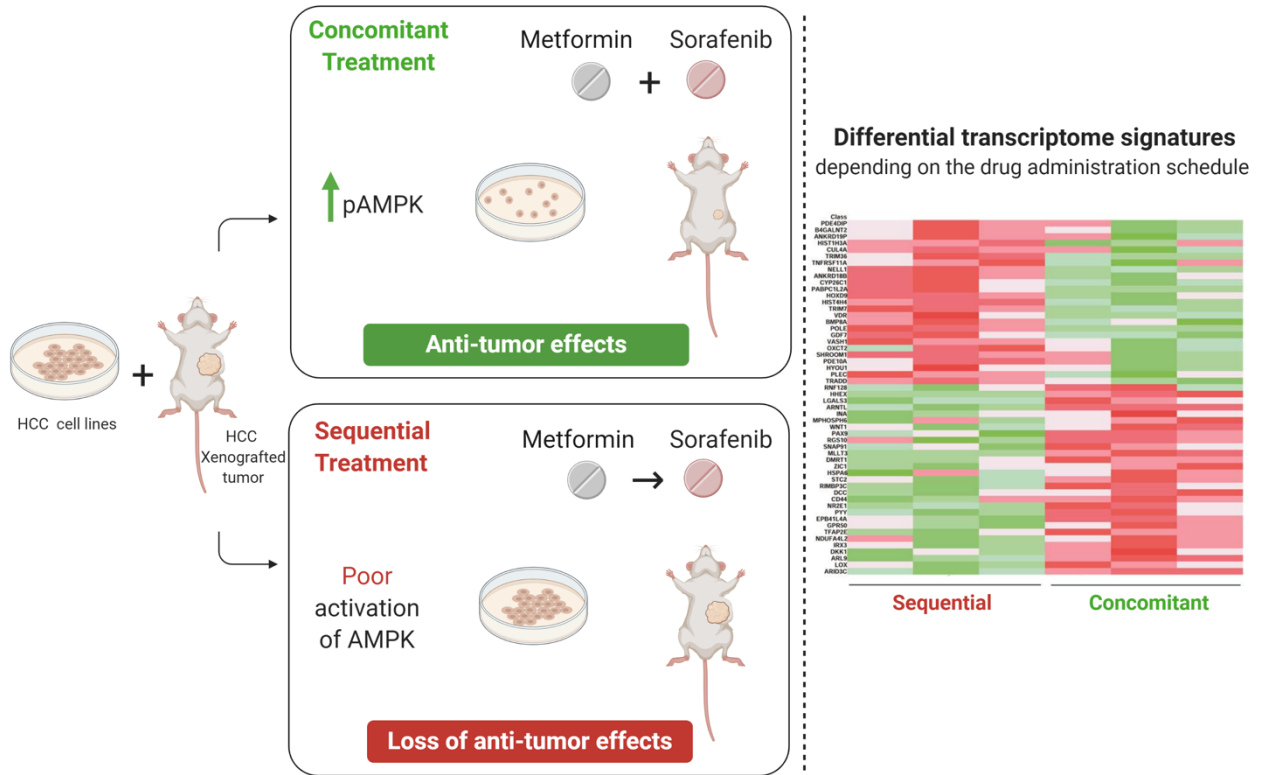
3. Abstract

Hepatocellular carcinoma (HCC) is the most common primary liver malignancy and is one of the leading causes of cancer-related deaths worldwide. The multi-target inhibitor sorafenib is a first-line treatment for patients with advanced unresectable HCC. Recent clinical studies have evidenced that patients treated with sorafenib together with the anti-diabetic drug metformin have a survival disadvantage compared to patients receiving sorafenib only. Here, we examined whether a clinically relevant dose of metformin (50 mg/kg/d) could influence the antitumoral effects of sorafenib (15 mg/kg/d) in a subcutaneous xenograft model of human HCC growth using two different sequences of administration, *i.e* concomitant *versus* sequential dosing regimens. We observed that the administration of metformin six hours prior to sorafenib was significantly less effective in inhibiting tumor growth than concomitant administration of the two drugs. *In vitro* experiments confirmed that pretreatment of different human HCC cell lines with metformin reduced the effects of sorafenib on cell viability, proliferation and signaling. Transcriptomic analysis confirmed significant differences between xenografted tumors obtained under the concomitant and the sequential dosing regimens. Taken together, these observations call into question the benefit of parallel use of metformin and sorafenib in patients with advanced HCC and diabetes, as the interaction between the two drugs could ultimately compromise patient survival.

4. Significance statement

When drugs are administered sequentially, metformin alters the anti-tumour effect of sorafenib, the reference treatment for advanced hepatocellular carcinoma, in a preclinical murine xenograft model of liver cancer progression as well as in hepatic cancer cell lines. Defective activation of the AMPK pathway as well as major transcriptomic changes are associated with the loss of the anti-tumour effect. These results echo recent clinical work reporting a poorer prognosis for patients with liver cancer who were co-treated with metformin and sorafenib.

5. Visual abstract



Created with BioRender

6. Introduction

Primary liver cancer ranks at the sixth and fourth positions in terms of incidence and mortality, respectively and hepatocellular carcinoma (HCC) accounts for 90% of cases (Ferlay et al., 2019). Treatment options for HCC are limited and outcomes remain poor, especially for unresectable advanced tumors. The multi-target inhibitors sorafenib and lenvatinib have been approved as first-line treatments for patients with advanced HCC. These therapies have demonstrated significant but modest effects on overall survival (Yarchoan et al., 2019).

These last years, the etiological and epidemiological landscape of HCC has undergone significant changes. While chronic viral hepatitis B and C and massive alcohol consumption have been the major etiological factors for decades, the worldwide epidemic of obesity and type 2 diabetes (T2D) has revealed that these metabolic diseases are involved in the pathogenesis of HCC, due to their ability to induce metabolic-associated steatohepatitis (MASH). MASH is becoming the leading etiology underlying many cases of HCC, especially in industrialized countries (Anstee et al., 2019; Younossi et al., 2019).

Metformin, a widely used oral biguanide for T2D treatment, has been associated with a lower risk of HCC among diabetic patients (Cunha et al., 2020; Zhou et al., 2016) and with increased survival among HCC patients treated with surgery (Schulte et al., 2019). In contrast, recent clinical studies have raised doubt about the efficacy of metformin and sorafenib administration in diabetic patients with advanced HCC. Indeed, it has been reported that patients treated with sorafenib have a survival disadvantage when they are treated with metformin, their overall survival being 4-5 months shorter compared to patients receiving sorafenib only (Casadei Gardini et al., 2017; Casadei Gardini et al., 2015; Schulte et al., 2019).

Up to now, experimental studies performed in murine models of HCC and designed to examine the antitumor effects of metformin in the presence of sorafenib have not been able to substantiate pharmacokinetic or pharmacodynamic drug-drug interaction. It has been reported that the concomitant administration of metformin with sorafenib (30 mg/kg/d) was more efficient than monotherapies to inhibit growth and metastatic dissemination of orthotopically engrafted MHCC97H cells (Guo et al., 2016; You et al., 2016). The metformin and sorafenib combination also led to growth inhibition of subcutaneously xenografted Bel-7402 cells compared to single agent (Ling et al., 2017). However, it is important to note that these studies were conducted with a high dose of metformin (200 mg/kg/d), which is not consistent with the therapeutic doses achievable in diabetic patients (33-42 mg/kg/d). In addition, drugs were administered according to a single regimen, *i.e* concomitant administration.

In this context, the present report was designed to examine whether a clinically relevant dose of metformin (50 mg/kg/d) has antitumoral effects when co-administrated with sorafenib (15 mg/kg/d) in a subcutaneous xenograft model of human HCC growth. Two different sequences of administration were tested for metformin and sorafenib, *i.e.* concomitant *versus* sequential. While metformin alone was ineffective to prevent or slow down the growth of tumor cell xenografts, we observed that the antitumoral efficacy of the combination of metformin with sorafenib was influenced by the treatment time schedule. Indeed, the administration of metformin six hours prior to sorafenib was significantly less efficient to impair tumor growth than the concomitant administration of the two drugs. *In vitro* experiments confirmed that cell pretreatment with metformin reduced the effect of sorafenib on cell viability, proliferation and signaling in a panel of HCC cell lines. A transcriptomic analysis confirmed significant differences between xenografted tumors obtained under concomitant and sequential dosing regimens.

Overall, these observations might have important implications for the therapeutic management of diabetic patients with unresectable HCC.

7. Materials and methods

Pharmacological drugs. Sorafenib (*p*-toluene sulfonate salt) was purchased from LC Laboratories (Woburn, MA, USA), and metformin was from Sigma-Aldrich (Saint-Quentin Fallavier, France). For *in vitro* studies, sorafenib and metformin were dissolved in dimethylsulfoxide (Sigma-Aldrich Chemie S.a.r.l., Saint-Quentin Fallavier, France) and serum-free medium, respectively. For *in vivo* studies, sorafenib and metformin were dissolved in Cremophor EL/ethanol/water (12.5%:12.5%:75%, Sigma-Aldrich) and sterile water, respectively. AICAR (*N*1-(β -DRibofuranosyl)-5-aminoimidazole-4-carboxamide) was from Tocris Bioscience (Bio-Techne Europe, Lille, France).

Xenografts. All *in vivo* experiments were conducted in compliance with the European regulations and ethical guidelines for experimental animal studies. Six week-old female athymic mice (Rj:NMRI-Foxn1nu/Foxn1nu, Janvier Labs, Le Genest-Saint-Isle, France) were inoculated *s.c.* in the right flank with 2×10^6 PLC/PRF5 cells suspended in 50% Matrigel (BD Biosciences, San Jose, CA). Tumor size was measured thrice a week using a hand caliper and tumor volume was calculated using the formula: length x (width)² x 0.52. Mice were treated by gavage with vehicles (control), sorafenib alone (15 mg/kg/day), metformin alone (50 mg/kg/day), metformin combined to sorafenib (concomitant schedule) and metformin followed 6 h later by sorafenib (sequential schedule). Mice were weighed thrice a week to follow drug toxicity. Weight loss greater than 15% was considered as a sign of toxicity. After 15 days, mice were anesthetized and tumors were excised, flash frozen in liquid nitrogen and stored at -80°C for further analyses.

Plasma concentrations of metformin and sorafenib. Plasma concentrations of sorafenib were determined 2 h and 6 h post-administration by gavage using a previously described high-performance liquid chromatography method (Blanchet et al., 2009). The accuracy, within-assay and between assay precision of this method were 96.9–104.0%, 3.4–6.2% and 7.6–9.9%, respectively. Plasma concentrations of metformin were determined using a modified ultra high-pressure liquid chromatography assay with UV DAD (diode array detector) as previously described (Jeyabalan et al., 2013).

Cell culture and treatments. HepG2, Hep3B, and Huh7 cells were obtained from the American Type Culture Collection (ATCC). PLC/PRF5 and Huh6 cells were provided by Dr Christine Perret (Institut Cochin, France). Cell line authentication was performed by using a panel of nine short tandem repeats as previously reported (Goumard et al., 2017). Cell lines were cultured as reported elsewhere (Blivet-Van Eggelpoel et al., 2012) and routinely controlled for mycoplasma contamination. Human hepatocytes in primary culture were obtained as reported elsewhere (Aoudjehane et al., 2016).

Cell viability and proliferation. Cell viability was evaluated using the 3-(4,5-dimethylthiazol-2-yl)-2,5-diphenyltetrazolium bromide assay (MTT assay) as previously reported (Desbois-Mouthon et al., 2009). Cell proliferation was evaluated by direct cell counting and by staining DNA with 0.1% crystal violet in 20% methanol during 30 min at room temperature with gentle shaking. Crystal violet dye was extracted using 10% SDS, 0.01 mM HCl at 37°C during 1 h and absorbance was determined at 570 nm in a microplate reader (Infinite F200 PRO, Tecan, Switzerland).

Western blotting. Protein electrophoresis and transfer to nitrocellulose were performed according to standard procedures using primary antibodies against phospho-AMPK α (Thr172) (40H9), AMPK α (Cell Signaling Technology Europe, Leiden, Netherlands) and β -actin (AC-15) (Sigma-Aldrich). Blot revelations were performed using ChemiDocTM Touch Imaging System (BIO-RAD, Hercules, CA, USA).

RNA isolation and analysis of gene expression. Total RNA was extracted from cell cultures using Nucleospin RNA kit (Macherey-Nagel SARL, Hoerd, France). Quantitative measurements of transcripts were performed by real-time PCR on a LightCycler 96 instrument (Roche Diagnostics, Meylan, France) using SYBR Green chemistry and specific primers for *ABCB1* (coding for MDR1/PgP) (forward: 5'-GAAATTTAGAAGATCTGATGTCAAACA-3', reverse: 5'-ACTGTAATAATAGGCATACCTGGTCA-3'), *ABCG2* (coding for *BCRP*) (forward: 5'-TGGCTTAGACTCAAGCACAGC-3', reverse: 5'-TCGTCCCTGCTTAGACATCC-3'), *RALBP1* (coding for RLIP76) (forward: 5'-CGGCTCTCTCGCTGTACATT-3', reverse: 5'-GAACCTGAGCCTGACGTGAA-3'), *SLC22A1* (coding for OCT1) (forward: 5'-CTGAGGGAGACATTGCACCT-3', reverse: 5'-TGCTCCAGAATGTCATCCAC-3'), *SLCO1B1* (coding for OATP1B1) (forward: 5'-GGGTGGACTTGTTGCAGTTG-3', reverse: 5'-TGTTTTTGTGTTGATGCTCAGT-3'), and *SLCO1B3* (coding for OATP1B3) (forward: 5'-TCAAGTGGTATTA AAAAGCATA CAGTG-3', reverse: 5'-TTCACCCAAGTGTGCTGAGT-3'). For each sample, gene expression was normalized to that of hypoxanthine guanine phosphoribosyltransferase mRNA content (forward: 5'-TAATTGGTGGAGATGATCT-3', reverse: 5'-TGCCTGACCAAGGAAAGC-3'). The relative quantity of each target gene was determined from replicate samples using the formula $2^{-\Delta\Delta Ct}$.

Uptake of radiolabeled sorafenib. HCC cells (7×10^4 cells/well) grown in 24-well plates were preincubated for 30 minutes at 37°C in uptake buffer (96 mM NaCl, 5.3 mM KCl, 1.1 mM KH₂PO₄, 0.8 mM MgSO₄, 1.8 mM CaCl₂, 11 mM D-glucose, 50 mM HEPES, pH 7.4). Experiments were initiated by replacement of uptake medium with 0.5 ml of 0.2 µCi/mL [³H]sorafenib (Moravek Inc., Brea, CA, USA) in uptake buffer. Initially, time-dependent experiments were conducted for up to 20 minutes to determine the linear uptake range (unpublished data). After incubation, radioactive solutions were aspirated and cells were washed four times with 4°C uptake buffer. Cells were lysed with 500 µL of 0.1 N NaOH/0.1% SDS for 4 hours, and samples were analyzed by liquid scintillation counting. Data were normalized to protein concentration determined using BCA protein assay reagent kit.

Gene expression microarray. Total RNA was extracted using Trizol (ThermoFischer Scientific) from tumors collected from mice xenografted and treated with vehicle (control, n=3), metformin (50 mg/kg/day) combined to sorafenib (15 mg/kg/day) (concomitant schedule, n=3) or metformin (50 mg/kg/day) followed 6 hours later by sorafenib (15 mg/kg/day) (sequential schedule, n=3). RNA integrity was assessed using the Agilent 2100 Bioanalyzer (Agilent Technologies, Palo Alto, CA, USA). Total RNA was amplified and labelled using the GeneChip™ WT PLUS Reagent Kit (ThermoFischer Scientific). Each RNA sample was hybridized to Human Clariom™ S GeneChip (ThermoFischer Scientific). Arrays were scanned, and images were analyzed and controlled for hybridization artefacts.

Microarray analysis. The microarray data were normalized using Signal Space Transformation-RMA (SST-RMA) which is optimized for under-estimation of true fold changes (Irizarry et al., 2003). Following normalization, differential expression was carried out using eBayes function and One-Way Anova statistical analysis. The analysis was carried out using Transcriptome Analysis Console software (ThermoFischer Scientific, version 4.0.2) with $p < 0.05$ considered as statistically significant. The differentially expressed genes were then subjected to absolute GSEA searching through more than 10,000 different cellular pathways as described in Hamoudi *et al.* (Hamoudi et al., 2010). C2 is an MSigDB (The Molecular Signature Database) collection consisting of sets curated from biomedical literature and online pathway databases such as the Kyoto Encyclopedia of Genes and Genome (KEGG) (Kanehisa and Goto, 2000) or Reactome (Croft et al., 2011). The gene ontology set C5 contains curated sets derived from Gene Ontology (Ashburner et al., 2000). The data discussed in this publication have been deposited in NCBI's Gene Expression Omnibus and are accessible through GEO series accession number GSE162557.

Statistical Analysis. Statistical analyses were performed using GraphPad Prism software (San Diego, USA). Values are presented as mean \pm SEM. Comparisons were performed using nonparametric tests (Mann-Whitney test for two-group comparisons and Kruskal-Wallis test if more than two groups were compared; the Dunn's test was used as a post hoc test). Differences were considered statistically significant at $p < 0.05$.

8. Results

***In vivo* effects of a clinically-relevant dose of metformin in combination with sorafenib on HCC growth**

A low dose of metformin (50 mg/kg/d) was administered by gavage in the following experiments. This dose which is comparable with that used in metformin-treated diabetic patients (33.3-42.5 mg/kg/d), has been reported to reduce insulin resistance and to normalize glycemia in diabetic mice (Foretz et al., 2010). We confirmed that the intra-gastric administration of 50 mg/kg/d metformin to nude mice led to metformin plasma concentrations that reached 0.55 ± 0.18 mg/L two hours after administration (**Table 1**), which was close to the therapeutic values observed in humans (Lalau et al., 2011).

The first set of experiments was designed to evaluate the effect of the low dose of metformin alone on tumor growth in a model of subcutaneously xenografted PLC/PRF5 cells. Metformin and vehicle administration was initiated four days before HCC cell grafts and was maintained during the next 15 days. We observed that 50 mg/kg/d metformin altered neither tumor initiation (100% of mice developed tumors), nor the kinetics of tumor growth in comparison with the control group (**Figure S1**).

In the second set of experiments, the ability of 50 mg/kg/d metformin to improve the antitumoral effect of sorafenib was evaluated on established xenografted tumors (~250 mm³). A dose of 15 mg/kg/d sorafenib was used in these experiments, which is equivalent to that used in humans for the treatment of advanced HCC (800 mg/d). This dose led to plasma sorafenib concentrations of 2.52 ± 1.03 mg/L two hours post administration in nude mice (**Table 1**) (therapeutic concentrations in humans: 2-5 mg/L). In order to define the optimal sequence, two administration schedules were

followed: metformin was administrated concomitantly to sorafenib (concomitant schedule) or 6 hours before sorafenib (sequential schedule). Groups of mice receiving vehicle, sorafenib or metformin alone were run in parallel. As shown on **Figure 1a** and **Table 2**, 15 mg/kg/d sorafenib alone significantly reduced by 42.3% tumor volume as compared to the control group. When metformin and sorafenib were administrated concomitantly, tumor volumes tended to be smaller than those obtained with sorafenib alone (59.5% tumor growth inhibition as compared to the control group). In contrast, the sequential therapy had no significant antitumor effect. The analysis of tumor masses at sacrifice confirmed that the sequential schedule was not effective to reduce tumor mass (**Figure 1b**). None of the different treatments showed toxicity as monitored by body weight evaluation (data not shown). Altogether, these data indicate that metformin has schedule-dependent antitumor effects against HCC cells when combined with sorafenib; the sequential schedule (administration of metformin 6 h before sorafenib) seems to impair the anticancer activity of sorafenib.

Effects of metformin on plasma concentrations of sorafenib

To approach the potential mechanisms accounting for metformin-mediated inhibition of sorafenib effect, we first measured plasma concentrations of sorafenib. Plasma concentrations were measured in mice treated concomitantly with sorafenib and metformin during 2 h or 6 h and in mice pretreated with metformin during 2 h or 4 h and then exposed to sorafenib during 2 h. As shown in **Table 1**, the concomitant and sequential administrations of metformin did not modify the average plasmatic concentrations of sorafenib as compared to that obtained in mice treated with sorafenib alone.

***In vitro* effects of metformin in combination with sorafenib on HCC cell viability and proliferation**

We then analysed the effects of metformin and sorafenib on the viability of the PLC/PRF5 cell line using an *in vitro* MTT assay. As shown in **Figures 2a** and **2b**, the concomitant treatment of PLC/PRF5 cells with suboptimal concentrations of metformin and sorafenib decreased cell viability to a larger extent than did each drug alone. In contrast, the sequential treatment (pre-treatment with metformin during 6 h) was significantly less effective to reduce cellular viability than the concomitant treatment. We extended analyses to three human other liver cancer cell lines, namely Hep3B, HepG2 and Huh7. In these three cell lines, the concomitant combination of metformin with sorafenib was significantly more efficient to reduce cell viability than was the sequential schedule (**Figure 2a**).

As metformin is known to affect the mitochondrial complex 1 of the respiratory chain, it might interfere with the MTT assay, which relies on mitochondrial activity. Therefore, we also evaluated the effects of concomitant and sequential treatments on HCC cell proliferation using two assays that do not rely on cell functionalities. As shown in **Figures 3a** and **3b**, the concomitant treatment was more potent than the sequential schedule to reduce proliferation in PLC/PRF5 and Huh7 cells evaluated both by cell counting and DNA staining with crystal violet. Altogether, these data support the conclusion that when metformin was administrated before, the antiproliferative effect of sorafenib was reduced *in vitro*.

Effects of metformin on sorafenib uptake in HCC cells

We then investigated whether metformin may alter sorafenib uptake in HCC cells. Sorafenib uptake has been reported to occur *via* both passive (Hu et al., 2009; Swift

et al., 2013) and active (Herraez et al., 2013; Swift et al., 2013; Zimmerman et al., 2013) diffusion in different cell types. The active portion may involve organic anion-transporting polypeptides (OATPs) 1B1 and 1B3 and organic cation transporter-1 (OCT1). As shown in **Figure 4a**, hepatic cancer cell lines exhibited low levels of OATP1B1, OATP1B3 and OCT1 transcripts compared to normal human hepatocytes. Cell treatment with metformin (1 mM, 24 h) had no effect on mRNA expression of influx transporters (data not shown).

Efflux clearance of sorafenib has been shown to be mediated by different transporters. BCRP/ABCG2 functions as an efflux pump for sorafenib *in vivo* in mouse brain (Agarwal and Elmquist, 2012; Agarwal et al., 2011; Tang et al., 2013) and *in vitro* in MDCKII and Hep3B cells (Huang et al., 2013; Poller et al., 2011). RLIP76, a stress-responsive membrane protein, has been identified as a transporter for sorafenib in kidney cancer cells (Singhal et al., 2010). In contrast, sorafenib seems to be a weak substrate for Pgp/MDR1/ABCB1 *in vitro* in the K562/Dox cell line (Haouala et al., 2010) and *in vivo* in mouse (Agarwal and Elmquist, 2012). These three pumps were expressed differentially in HCC cell lines (**Figure 4b**) and cell treatment with metformin (1 mM, 24 h) was without any effect on mRNA expression of efflux transporters (data not shown).

We examined whether cell pretreatment with metformin may impact drug uptake using radiolabeled [³H]sorafenib. Experiments were performed at 37°C and also at 4°C to assess the contribution of passive diffusion to overall uptake. The uptake of [³H]sorafenib at 4°C was reduced by 58% compared with 37°C confirming a substantial degree of passive diffusion (**Figure 4c**). At both temperatures, cell pretreatment with metformin during six hours did not alter sorafenib cellular accumulation (**Figure 4c, d**).

These data did not support for a role of metformin on the regulation of sorafenib disposal into HCC cells *in vitro*.

***In vitro* effects of metformin in combination with sorafenib on AMPK phosphorylation**

The combination of metformin and sorafenib has been reported to be synergistic in non-small cell lung cancer cells through AMP-activated protein kinase (AMPK) activation (Groenendijk et al., 2015). Therefore, we next investigated whether sequential and concomitant regimens differentially affected the AMPK pathway. Using AICAR which is a cell permeable activator of AMPK (through its phosphorylation) in different cancer cell lines including HCC cells (Cheng et al., 2014), we observed that the concomitant treatment of PLC/PRF5 and Huh7 cells with AICAR and sorafenib reduced cell viability more efficiently than drugs alone while the sequential treatment turned to be less potent (**Figure 5a**). These data mimic those obtained with the metformin/sorafenib combinations (**Figure 2**) and suggest that the cross-resistance observed between metformin and sorafenib in the sequential schedule may be associated with an inadequate stimulation of AMPK activity. To test this hypothesis, the phosphorylation level of AMPK was examined by Western blot analysis in the different cell lines treated during 24 h with drugs alone, drugs in combination or with metformin during 6 h followed by sorafenib for the next 18 h. As shown in **Figure 5b**, the concomitant treatment increased phospho-AMPK in comparison with control and monotherapies while the sequential treatment led to a lower activation of AMPK phosphorylation.

Genes differentially expressed in concomitant and sequential regimens

To better characterize the molecular signatures driving the differential responses to concomitant and sequential bitherapies, we conducted a transcriptomic analysis on RNA extracted from tumor xenografts. Using Anova to filter differentially expressed genes obtained from eBayes function, 1035 genes were identified to be differentially expressed between control and concomitant treatments, 771 genes between control and sequential treatments and 1051 between sequential and concomitant treatments. Among these differentially expressed genes, 193 were commonly altered by both types of treatments (sequential and concomitant) while 842 genes were altered by the concomitant treatment only and 578 genes by the sequential treatment (**Figure 6a**).

The differentially expressed genes were subjected to absolute GSEA searching through more than 10,000 different cellular pathways (**Figure 6b**). The analysis identified 6 and 24 pathways derived from the C2 and C5 gene sets respectively as differentially expressed between the control and concomitant treatments, while 15 and 18 pathways derived from the C2 and C5 gene sets respectively were differentially expressed between the control and sequential treatments (**Tables S1 and S2**). Ten pathways derived from C2 gene sets and 5 pathways from C5 gene sets were differentially expressed between concomitant and sequential treatments (**Table S3**).

Some of the pathways identified for the concomitant treatment are related to G-proteins coupled receptors (GPCR) and transmembrane receptors signaling such as GO_G_PROTEIN_COUPLED_RECEPTOR_ACTIVITY (GO:0007186) and GO_TRANSMEMBRANE_SIGNALING_RECEPTOR_ACTIVITY (GO:0004888). Some of the pathways identified for the sequential treatment are related to protein kinases, receptor tyrosine kinases (RTKs) and mitogen-activated protein kinase (MAPK) signaling such as REACTOME SIGNALING BY RECEPTOR TYROSINE KINASES (R-HSA-9006934), POSITIVE REGULATION OF MAPK CASCADE

(GO:0043410) and
GO_REGULATION_OF_PHOSPHORUS_METABOLIC_PROCESS (GO:0051174).
Some of the pathways differentially expressed between sequential and concomitant
treatments are also related to GPCR such as REACTOME_SIGNALING_BY_GPCR
(R-HSA-372790), REACTOME_GPCR_LIGAND_BINDING (R-HSA-500792),
GO_G_PROTEIN_COUPLED_RECEPTOR_ACTIVITY (GO:0004930) as well as cell
proliferation such as BENPORATH_EED_TARGETS (M7617) (**Figure 6c**).

For each significant pathway, the enriched genes were identified and their
recurrence in other pathways was searched as previously described (Hamoudi et al.,
2010). The genes detected in more than three different pathways were considered of
significance for the drug mechanism of action (**Table S4**). Applying this approach to
concomitant drug treatment, 11 members of the olfactory receptors family (such as
OR10H3 and *OR7G1*) as well as other genes such as *CEACAM1*, *SCN1A*, and
ADAM8 amongst others were found significantly overexpressed in treated tumors
compared to untreated control tumors (*OR10H3*: fold change = 1.38, $p = 0.0228$;
OR11G2 : fold change = 1.29, $p = 0.0175$; *OR13D1*: fold change = 1.33, $p = 0.0347$;
CEACAM1: fold change = 2.84, $p = 0.0009$; *ADAM8*: fold change = 1.65, $p = 0.017$)
while 7 members of the olfactory receptors family (such as *OR2AG2* and *OR2T10*)
were down-regulated (*OR2AG2*: fold change = -1.43, $p = 0.0173$; *OR2T10*: fold change
= -1.35, $p = 0.0137$).

In sequential treatment, *PRKAR1A*, *STAT3*, *STAT5B*, *IRS2*, *AKT2* and *CEACAM1*
were overexpressed in treated tumors (*PRKAR1A*: fold change = 1.68, $p = 0.0254$;
STAT3: fold change = 1.18, $p = 0.03$; *STAT5B*: fold change = 1.33, $p = 0.0135$; *IRS2*:
fold change = 2.01, $p = 0.0212$; *AKT2*: fold change = 1.42, $p = 0.0163$; *CEACAM1*: fold

change = 1.71, $p = 0.0304$) while *FGF2* and *CCL20* were downregulated amongst others (*FGF2*: fold change = -1.55, $p = 0.02$; *CCL20*: fold change = -1.91, $p = 0.002$).

Comparing the two modes of treatments, genes detected in more than three pathways and upregulated in sequential treatment compared to concomitant include *PDE4DIP* (fold change = 1.91, $p = 0.0245$), while downregulated genes include *PYY* (fold change = -1.55, $p = 0.0036$) and *WNT1* (fold change = -1.24, $p = 0.0389$).

Altogether these data substantiate the notion that the combination of metformin and sorafenib according to sequential and concomitant regimens leads to qualitatively and quantitatively different signaling pathways in HCC tumors that may account for differential antitumor responses.

9. Discussion

In the present study, we investigated the underlying mechanisms that may account for the clinical finding that patients receiving both metformin and sorafenib have reduced survival compared to patients receiving sorafenib alone (Casadei Gardini et al., 2017; Casadei Gardini et al., 2015; Schulte et al., 2019). Using a xenograft model of HCC growth, we identified a differential therapeutic response to the bitherapy metformin/sorafenib depending upon the drug administration schedule (concomitant *versus* sequential) and provide novel insights into the complex and interactive molecular mechanism of the metformin/sorafenib combination.

Sorafenib is the gold standard, first-line systemic treatment for advanced HCC since 2007. It provides a modest but significant survival benefit over placebo (Marisi et al., 2018). Sorafenib is a multi-kinase inhibitor targeting Raf kinase activity, STAT3-dependent signaling and RTKs such as vascular endothelial growth factor receptor, platelet-derived growth factor receptor- β and c-KIT (Tai et al., 2011; Wilhelm et al., 2008). These pleiotropic actions confer to sorafenib potential inhibitory effects on tumor cell proliferation and neovascularization.

Because of its great potency to reduce liver glucose production, its relatively low cost and its safety profile even in case of cirrhosis (Bhat et al., 2014; Zhang et al., 2014), metformin is the first medication prescribed to patients with T2D. Several studies have also reported a preventive role of metformin on HCC development among diabetic patients (Cunha et al., 2020; Zhou et al., 2016). This is thought to be related to the glucose-lowering and insulin-sensitizing effects of metformin which might reduce the proliferation rate of premalignant hepatic lesions that thrive in high-glucose and/or high-

insulin environment. In addition, direct antitumor effects of metformin have been reported *in vitro* in HCC cells (Hu et al., 2019; Miyoshi et al., 2014; Tsai et al., 2017).

Recent observational clinical studies have cast doubt on the benefits for patients with HCC and diabetes to be treated simultaneously with sorafenib and metformin. Indeed, it has been reported that the use of sorafenib and metformin in patients with advanced HCC was associated with a poorer prognosis compared to the use of sorafenib alone (Casadei Gardini et al., 2017; Casadei Gardini et al., 2015; Schulte et al., 2019). These results were rather unexpected as preclinical experimental data were encouraging showing that the concomitant administration of metformin to sorafenib was more efficient than drugs alone to inhibit HCC tumor growth as well metastatic dissemination in immunodeficient mice bearing xenografts of human HCC cells (Guo et al., 2016; Ling et al., 2017; You et al., 2016). However, one limitation of these studies is that metformin was used at a high concentration (>200 mg/kg/d) generally unachievable in diabetic patients.

Therefore, we conducted the present study to re-evaluate the antitumor potential of the combination metformin/sorafenib, taking into account not only the dose of metformin used but also the drug administration regimen. In contrast to the results reported with high doses of metformin (Cauchy et al., 2017; Chen et al., 2013; Saito et al., 2013; Zheng et al., 2013), we observed that a low dose of metformin (50 mg/kg/d) was unable to inhibit the growth of established tumors in a HCC xenograft model. In this model, the co-administration of sorafenib with a low dose of metformin induced a significant reduction in tumor volume and mass compared to control but was not more effective than sorafenib monotherapy. Taken together, these data suggest that the antitumor effect of metformin cannot be achieved *in vivo* at a clinically-relevant dose.

Intriguingly, the sequential administration of metformin 6 h prior to sorafenib significantly impaired the anti-cancer effect of sorafenib on tumor growth in the HCC xenograft model. These observations were reproduced *in vitro* using a panel of four human HCC cell lines known to be genetically and phenotypically different (Caruso et al., 2019), which supports the relevance of our findings. Cell pretreatment with metformin impaired sorafenib effects on HCC cell viability and proliferation *in vitro*. Furthermore, prior administration of metformin impacted neither the plasma concentrations of sorafenib 2 and 6 h after its administration, nor the intracellular bioavailability of sorafenib in HCC cells *in vitro*. These results suggest a lack of pharmacokinetic interaction between metformin and sorafenib. Nevertheless, Karbownik and colleagues (Karbownik et al., 2020) recently reported a 40% decrease of the area under the plasma concentration-time curve of sorafenib (without modifying maximal plasma concentration) in rats receiving concomitantly a single dose of sorafenib (100 mg/kg) and metformin (100 mg/kg). The difference in animal models and doses of sorafenib and metformin between the two studies can explain the discrepancies of results. Overall, our observations suggest that the repressive effect of metformin on sorafenib action could be rather related to a pharmacodynamic interaction than a pharmacokinetic one. Further studies are warranted to further investigate this point.

The sequential use of metformin and sorafenib led to a poorer activation of AMPK in HCC cell lines than did the concomitant treatment. Metformin alone has been reported to exert some of its anti-cancer effects in HCC cells through the activation of AMPK and the subsequent inhibition of mTOR signaling (Cheng et al., 2014; Zheng et al., 2013). In addition, low levels of AMPK signaling has been associated with HCC cell resistance to sorafenib (Bort et al., 2019). Together with our *in vitro* findings

showing that cell pre-treatment with AICAR, another AMPK inhibitor, impaired HCC cell response to sorafenib, these data sustain the hypothesis that the deficit in AMPK signaling as evidenced in HCC cells pre-treated with metformin participates to tumor cell resistance to sorafenib.

The microarray analysis performed on RNA extracted from tumor xenografts confirmed that gene expression and cellular pathways are differentially altered by sequential and concomitant treatments with metformin and sorafenib. Of interest, pathways altered by the concomitant treatment mainly involve GPCRs that may account for the beneficial effect of the concomitant administration observed *in vivo* compared to sequential. GPCRs are known to increase intracellular levels of cAMP by activating adenylate cyclase which may concur to the subsequent stimulation of PKA, LKB1 and AMPK. In contrast, the sequential regimen rather altered pathways involving RTKs (*IRS2* and *AKT2* overexpression), STAT signaling (*STAT3* and *STAT5B* overexpression) and perturbation of cAMP signaling (*PRKAR1A*) that may account for its lack of efficacy compared to the concomitant administration. *PRKAR1A* codes for the type 1 α regulatory subunit of PKA and its overexpression has been reported in different cancer cell types. Downregulation of *PRKAR1A* in cancer cells with siRNA was shown to activate PKA through release of the catalytic subunit from the holoenzyme (Nadella et al., 2008).

The transcriptomic analysis also showed that both regimens induce expression of genes associated with therapeutic resistance and tumor progression. Regarding the sequential treatment, microarray analysis identified *FGF2* (*fibroblast growth factor 2*) and *CCL20* (*C-C motif chemokine ligand 20*) as downregulated after sequential treatment. *FGF2* downregulation could reduce elimination of HCC cells by natural killer-mediated innate immunity as previously reported (Tsunematsu et al., 2012) and

thus contributing to reduce treatment efficacy. As upregulation of *CCL20* was previously reported in sorafenib responders *versus* non responders (Covell, 2017), its downregulation is probably a marker of inefficacy of sequential combination. *CEACAM1* (*carcinoembryonic antigen-related cell adhesion molecule 1*) was upregulated in combinatory and sequential treatments and its upregulation has been associated with HCC invasion, progression and recurrence (Kiryama et al., 2014; Park et al., 2020; Yoshikawa et al., 2017). *ADAM8* (*ADAM metalloproteinase domain 8*) was overexpressed in concomitant treatment *versus* control. High expression of *ADAM8* was previously found to correlate with progression and poor prognosis in patients with HCC (Jiang et al., 2012; Zhang et al., 2013). These data suggest that despite its ability to target AMPK signaling, the combination metformin/sorafenib may also induce adverse signaling pathways that ultimately contribute to drug resistance and treatment failure, raising doubt about its benefit in the treatment of HCC.

In conclusion, our study provides important information on the molecular mechanisms of action of the metformin/sorafenib combination and suggests a pharmacodynamics drug interaction between the two molecules leading to a loss of antitumor activity. Our data call into question the benefit of parallel use of the two drugs in patients suffering from both advanced HCC and diabetes as this interaction could ultimately compromise patient survival.

10. Acknowledgements

The authors are greatly indebted to Corina Buta and Alkaly Gassama for their technical assistance. We thank Sébastien Jacques, Angéline Duché and Franck Letourneur from the platform GENOM'IC (Cochin Institute, INSERM U1016, Paris) for microarray experiments, Tatiana Ledent and the staff of the animal facility of the Saint-Antoine Research Center (INSERM UMR_S938).

11. Authorship contributions

Participated in Research design: Harati, Vandamme, Desbois-Mouthon

Conducted experiments: Harati, Vandamme, Desbois-Mouthon

Contributed new reagents or analytic tools: Blanchet, Bardin, Hamoudi

Performed data analysis: Harati, Vandamme, Hamoudi, Desbois-Mouthon

Wrote or contributed to the writing of the manuscript: Harati, Blanchet, Praz,
Hamoudi, Desbois-Mouthon

Funding acquisition: Harati, Desbois-Mouthon

12. References

- Agarwal S and Elmquist WF (2012) Insight into the cooperation of P-glycoprotein (ABCB1) and breast cancer resistance protein (ABCG2) at the blood-brain barrier: a case study examining sorafenib efflux clearance. *Molecular pharmaceutics* **9**(3): 678-684.
- Agarwal S, Sane R, Ohlfest JR and Elmquist WF (2011) The role of the breast cancer resistance protein (ABCG2) in the distribution of sorafenib to the brain. *The Journal of pharmacology and experimental therapeutics* **336**(1): 223-233.
- Anstee QM, Reeves HL, Kotsiliti E, Govaere O and Heikenwalder M (2019) From NASH to HCC: current concepts and future challenges. *Nature reviews Gastroenterology & hepatology* **16**(7): 411-428.
- Aoudjehane L, Boelle PY, Bisch G, Delelo R, Paye F, Scatton O, Housset C, Becquart J, Calmus Y and Conti F (2016) Development of an in vitro model to test antifibrotic drugs on primary human liver myofibroblasts. *Lab Invest* **96**(6): 672-679.
- Ashburner M, Ball CA, Blake JA, Botstein D, Butler H, Cherry JM, Davis AP, Dolinski K, Dwight SS, Eppig JT, Harris MA, Hill DP, Issel-Tarver L, Kasarskis A, Lewis S, Matese JC, Richardson JE, Ringwald M, Rubin GM and Sherlock G (2000) Gene ontology: tool for the unification of biology. The Gene Ontology Consortium. *Nat Genet* **25**(1): 25-29.
- Bhat M, Chaiteerakij R, Harmsen WS, Schleck CD, Yang JD, Giama NH, Therneau TM, Gores GJ and Roberts LR (2014) Metformin does not improve survival in patients with hepatocellular carcinoma. *World J Gastroenterol* **20**(42): 15750-15755.
- Blanchet B, Billefont B, Cramard J, Benichou AS, Chhun S, Harcouet L, Ropert S, Dauphin A, Goldwasser F and Tod M (2009) Validation of an HPLC-UV method for

- sorafenib determination in human plasma and application to cancer patients in routine clinical practice. *J Pharm Biomed Anal* **49**(4): 1109-1114.
- Blivet-Van Eggelpoel MJ, Chettouh H, Fartoux L, Aoudjehane L, Barbu V, Rey C, Priam S, Housset C, Rosmorduc O and Desbois-Mouthon C (2012) Epidermal growth factor receptor and HER-3 restrict cell response to sorafenib in hepatocellular carcinoma cells. *J Hepatol* **57**(1): 108-115.
- Bort A, Sanchez BG, Mateos-Gomez PA, Vara-Ciruelos D, Rodriguez-Henche N and Diaz-Laviada I (2019) Targeting AMP-activated kinase impacts hepatocellular cancer stem cells induced by long-term treatment with sorafenib. *Mol Oncol* **13**(5): 1311-1331.
- Caruso S, Calatayud AL, Pilet J, La Bella T, Rekik S, Imbeaud S, Letouze E, Meunier L, Bayard Q, Rohr-Udilova N, Peneau C, Grasl-Kraupp B, de Koning L, Ouine B, Bioulac-Sage P, Couchy G, Calderaro J, Nault JC, Zucman-Rossi J and Rebouissou S (2019) Analysis of Liver Cancer Cell Lines Identifies Agents With Likely Efficacy Against Hepatocellular Carcinoma and Markers of Response. *Gastroenterology* **157**(3): 760-776.
- Casadei Gardini A, Faloppi L, De Matteis S, Foschi FG, Silvestris N, Tovoli F, Palmieri V, Marisi G, Brunetti O, Vespasiani-Gentilucci U, Perrone G, Valgiusti M, Granato AM, Ercolani G, Negrini G, Tamburini E, Aprile G, Passardi A, Santini D, Cascinu S, Frassinetti GL and Scartozzi M (2017) Metformin and insulin impact on clinical outcome in patients with advanced hepatocellular carcinoma receiving sorafenib: Validation study and biological rationale. *Eur J Cancer* **86**: 106-114.
- Casadei Gardini A, Marisi G, Scarpi E, Scartozzi M, Faloppi L, Silvestris N, Masi G, Vivaldi C, Brunetti O, Tamperi S, Foschi FG, Tamburini E, Tenti E, Ricca Rosellini S, Ulivi P, Cascinu S, Nanni O and Frassinetti GL (2015) Effects of metformin on

- clinical outcome in diabetic patients with advanced HCC receiving sorafenib. *Expert Opin Pharmacother* **16**(18): 2719-2725.
- Cauchy F, Mebarki M, Leporq B, Laouirem S, Albuquerque M, Lambert S, Bourgoin P, Soubrane O, Van Beers BE, Faivre S, Bedossa P and Paradis V (2017) Strong antineoplastic effects of metformin in preclinical models of liver carcinogenesis. *Clin Sci (Lond)* **131**(1): 27-36.
- Chen HP, Shieh JJ, Chang CC, Chen TT, Lin JT, Wu MS, Lin JH and Wu CY (2013) Metformin decreases hepatocellular carcinoma risk in a dose-dependent manner: population-based and in vitro studies. *Gut* **62**(4): 606-615.
- Cheng J, Huang T, Li Y, Guo Y, Zhu Y, Wang Q, Tan X, Chen W, Zhang Y, Cheng W, Yamamoto T, Jing X and Huang J (2014) AMP-activated protein kinase suppresses the in vitro and in vivo proliferation of hepatocellular carcinoma. *PLoS One* **9**(4): e93256.
- Covell DG (2017) A data mining approach for identifying pathway-gene biomarkers for predicting clinical outcome: A case study of erlotinib and sorafenib. *PLoS One* **12**(8): e0181991.
- Croft D, O'Kelly G, Wu G, Haw R, Gillespie M, Matthews L, Caudy M, Garapati P, Gopinath G, Jassal B, Jupe S, Kalatskaya I, Mahajan S, May B, Ndegwa N, Schmidt E, Shamovsky V, Yung C, Birney E, Hermjakob H, D'Eustachio P and Stein L (2011) Reactome: a database of reactions, pathways and biological processes. *Nucleic Acids Res* **39**(Database issue): D691-697.
- Cunha V, Cotrim HP, Rocha R, Carvalho K and Lins-Kusterer L (2020) Metformin in the prevention of hepatocellular carcinoma in diabetic patients: A systematic review. *Ann Hepatol* **19**(3): 232-237.

- Desbois-Mouthon C, Baron A, Blivet-Van Eggelpoel MJ, Fartoux L, Venot C, Bladt F, Housset C and Rosmorduc O (2009) Insulin-Like Growth Factor-1 Receptor Inhibition Induces a Resistance Mechanism via the Epidermal Growth Factor Receptor/HER3/AKT Signaling Pathway: Rational Basis for Cotargeting Insulin-Like Growth Factor-1 Receptor and Epidermal Growth Factor Receptor in Hepatocellular Carcinoma. *Clinical Cancer Research* **15**(17): 5445-5456.
- Ferlay J, Colombet M, Soerjomataram I, Mathers C, Parkin DM, Pineros M, Znaor A and Bray F (2019) Estimating the global cancer incidence and mortality in 2018: GLOBOCAN sources and methods. *Int J Cancer* **144**(8): 1941-1953.
- Foretz M, Hebrard S, Leclerc J, Zarrinpashneh E, Soty M, Mithieux G, Sakamoto K, Andreelli F and Viollet B (2010) Metformin inhibits hepatic gluconeogenesis in mice independently of the LKB1/AMPK pathway via a decrease in hepatic energy state. *J Clin Invest* **120**(7): 2355-2369.
- Goumard C, Desbois-Mouthon C, Wendum D, Calmel C, Merabtene F, Scatton O and Praz F (2017) Low Levels of Microsatellite Instability at Simple Repeated Sequences Commonly Occur in Human Hepatocellular Carcinoma. *Cancer Genomics Proteomics* **14**(5): 329-339.
- Groenendijk FH, Mellema WW, van der Burg E, Schut E, Hauptmann M, Horlings HM, Willems SM, van den Heuvel MM, Jonkers J, Smit EF and Bernards R (2015) Sorafenib synergizes with metformin in NSCLC through AMPK pathway activation. *Int J Cancer* **136**(6): 1434-1444.
- Guo Z, Cao M, You A, Gao J, Zhou H, Li H, Cui Y, Fang F, Zhang W, Song T, Li Q, Zhu X, Sun H and Zhang T (2016) Metformin inhibits the prometastatic effect of sorafenib in hepatocellular carcinoma by upregulating the expression of TIP30. *Cancer Sci* **107**(4): 507-513.
- Hamoudi RA, Appert A, Ye H, Ruskone-Fourmestreaux A, Streubel B, Chott A, Raderer M, Gong L, Wlodarska I, De Wolf-Peeters C, MacLennan KA, de Leval L, Isaacson PG and Du MQ (2010) Differential expression of NF-kappaB target genes in MALT lymphoma with and

- without chromosome translocation: insights into molecular mechanism. *Leukemia* **24**(8): 1487-1497.
- Haouala A, Rumpold H, Untergasser G, Buclin T, Ris HB, Widmer N and Decosterd LA (2010) siRNA-mediated knock-down of P-glycoprotein expression reveals distinct cellular disposition of anticancer tyrosine kinases inhibitors. *Drug Metab Lett* **4**(2): 114-119.
- Herraez E, Lozano E, Macias RI, Vaquero J, Bujanda L, Banales JM, Marin JJ and Briz O (2013) Expression of SLC22A1 variants may affect the response of hepatocellular carcinoma and cholangiocarcinoma to sorafenib. *Hepatology* **58**(3): 1065-1073.
- Hu, Zeng Z, Xia Q, Liu Z, Feng X, Chen J, Huang M, Chen L, Fang Z, Liu Q, Zeng H, Zhou X and Liu J (2019) Metformin attenuates hepatoma cell proliferation by decreasing glycolytic flux through the HIF-1alpha/PFKFB3/PFK1 pathway. *Life Sci* **239**: 116966.
- Hu S, Chen Z, Franke R, Orwick S, Zhao M, Rudek MA, Sparreboom A and Baker SD (2009) Interaction of the multikinase inhibitors sorafenib and sunitinib with solute carriers and ATP-binding cassette transporters. *Clin Cancer Res* **15**(19): 6062-6069.
- Huang WC, Hsieh YL, Hung CM, Chien PH, Chien YF, Chen LC, Tu CY, Chen CH, Hsu SC, Lin YM and Chen YJ (2013) BCRP/ABCG2 inhibition sensitizes hepatocellular carcinoma cells to sorafenib. *PLoS One* **8**(12): e83627.
- Irizarry RA, Bolstad BM, Collin F, Cope LM, Hobbs B and Speed TP (2003) Summaries of Affymetrix GeneChip probe level data. *Nucleic Acids Res* **31**(4): e15.

- Jeyabalan J, Viollet B, Smitham P, Ellis SA, Zaman G, Bardin C, Goodship A, Roux JP, Pierre M and Chenu C (2013) The anti-diabetic drug metformin does not affect bone mass in vivo or fracture healing. *Osteoporos Int* **24**(10): 2659-2670.
- Jiang C, Zhang Y, Yu HF, Yu XT, Zhou SJ and Tan YF (2012) Expression of ADAM8 and its clinical values in diagnosis and prognosis of hepatocellular carcinoma. *Tumour Biol* **33**(6): 2167-2172.
- Kanehisa M and Goto S (2000) KEGG: kyoto encyclopedia of genes and genomes. *Nucleic Acids Res* **28**(1): 27-30.
- Karbownik A, Szkutnik-Fiedler D, Czyrski A, Kostewicz N, Kaczmarska P, Bekier M, Stanislawiak-Rudowicz J, Karazniewicz-Lada M, Wolc A, Glowka F, Grzeskowiak E and Szalek E (2020) Pharmacokinetic Interaction between Sorafenib and Atorvastatin, and Sorafenib and Metformin in Rats. *Pharmaceutics* **12**(7).
- Kiriyama S, Yokoyama S, Ueno M, Hayami S, Ieda J, Yamamoto N, Yamaguchi S, Mitani Y, Nakamura Y, Tani M, Mishra L, Shively JE and Yamaue H (2014) CEACAM1 long cytoplasmic domain isoform is associated with invasion and recurrence of hepatocellular carcinoma. *Ann Surg Oncol* **21 Suppl 4**: S505-514.
- Lalau JD, Lemaire-Hurtel AS and Lacroix C (2011) Establishment of a database of metformin plasma concentrations and erythrocyte levels in normal and emergency situations. *Clin Drug Investig* **31**(6): 435-438.
- Ling S, Song L, Fan N, Feng T, Liu L, Yang X, Wang M, Li Y, Tian Y, Zhao F, Liu Y, Huang Q, Hou Z, Xu F, Shi L and Li Y (2017) Combination of metformin and sorafenib suppresses proliferation and induces autophagy of hepatocellular carcinoma via targeting the mTOR pathway. *Int J Oncol* **50**(1): 297-309.
- Marisi G, Cucchetti A, Ulivi P, Canale M, Cabibbo G, Solaini L, Foschi FG, De Matteis S, Ercolani G, Valgiusti M, Frassinetti GL, Scartozzi M and Casadei Gardini A (2018)

Ten years of sorafenib in hepatocellular carcinoma: Are there any predictive and/or prognostic markers? *World J Gastroenterol* **24**(36): 4152-4163.

Miyoshi H, Kato K, Iwama H, Maeda E, Sakamoto T, Fujita K, Toyota Y, Tani J, Nomura T, Mimura S, Kobayashi M, Morishita A, Kobara H, Mori H, Yoneyama H, Deguchi A, Himoto T, Kurokohchi K, Okano K, Suzuki Y, Murao K and Masaki T (2014) Effect of the anti-diabetic drug metformin in hepatocellular carcinoma in vitro and in vivo. *Int J Oncol* **45**(1): 322-332.

Nadella KS, Jones GN, Trimboli A, Stratakis CA, Leone G and Kirschner LS (2008) Targeted deletion of Prkar1a reveals a role for protein kinase A in mesenchymal-to-epithelial transition. *Cancer Res* **68**(8): 2671-2677.

Park DJ, Sung PS, Kim JH, Lee GW, Jang JW, Jung ES, Bae SH, Choi JY and Yoon SK (2020) EpCAM-high liver cancer stem cells resist natural killer cell-mediated cytotoxicity by upregulating CEACAM1. *J Immunother Cancer* **8**(1).

Poller B, Wagenaar E, Tang SC and Schinkel AH (2011) Double-transduced MDCKII cells to study human P-glycoprotein (ABCB1) and breast cancer resistance protein (ABCG2) interplay in drug transport across the blood-brain barrier. *Molecular pharmaceutics* **8**(2): 571-582.

Saito T, Chiba T, Yuki K, Zen Y, Oshima M, Koide S, Motoyama T, Ogasawara S, Suzuki E, Ooka Y, Tawada A, Tada M, Kanai F, Takiguchi Y, Iwama A and Yokosuka O (2013) Metformin, a diabetes drug, eliminates tumor-initiating hepatocellular carcinoma cells. *PLoS One* **8**(7): e70010.

Schulte L, Scheiner B, Voigtlander T, Koch S, Schweitzer N, Marhenke S, Ivanyi P, Manns MP, Rodt T, Hinrichs JB, Weinmann A, Pinter M, Vogel A and Kirstein MM (2019) Treatment with metformin is associated with a prolonged survival in patients with hepatocellular carcinoma. *Liver Int* **39**(4): 714-726.

- Singhal SS, Sehrawat A, Sahu M, Singhal P, Vatsyayan R, Rao Lelsani PC, Yadav S and Awasthi S (2010) Rlip76 transports sunitinib and sorafenib and mediates drug resistance in kidney cancer. *Int J Cancer* **126**(6): 1327-1338.
- Swift B, Nebot N, Lee JK, Han T, Proctor WR, Thakker DR, Lang D, Radtke M, Gnoth MJ and Brouwer KL (2013) Sorafenib hepatobiliary disposition: mechanisms of hepatic uptake and disposition of generated metabolites. *Drug metabolism and disposition: the biological fate of chemicals* **41**(6): 1179-1186.
- Tai WT, Cheng AL, Shiau CW, Huang HP, Huang JW, Chen PJ and Chen KF (2011) Signal transducer and activator of transcription 3 is a major kinase-independent target of sorafenib in hepatocellular carcinoma. *Journal of hepatology* **55**(5): 1041-1048.
- Tang SC, de Vries N, Sparidans RW, Wagenaar E, Beijnen JH and Schinkel AH (2013) Impact of P-glycoprotein (ABCB1) and breast cancer resistance protein (ABCG2) gene dosage on plasma pharmacokinetics and brain accumulation of dasatinib, sorafenib, and sunitinib. *The Journal of pharmacology and experimental therapeutics* **346**(3): 486-494.
- Tsai HH, Lai HY, Chen YC, Li CF, Huang HS, Liu HS, Tsai YS and Wang JM (2017) Metformin promotes apoptosis in hepatocellular carcinoma through the CEBPD-induced autophagy pathway. *Oncotarget* **8**(8): 13832-13845.
- Tsunematsu H, Tatsumi T, Kohga K, Yamamoto M, Aketa H, Miyagi T, Hosui A, Hiramatsu N, Kanto T, Hayashi N and Takehara T (2012) Fibroblast growth factor-2 enhances NK sensitivity of hepatocellular carcinoma cells. *Int J Cancer* **130**(2): 356-364.
- Wilhelm SM, Adnane L, Newell P, Villanueva A, Llovet JM and Lynch M (2008) Preclinical overview of sorafenib, a multikinase inhibitor that targets both Raf and

VEGF and PDGF receptor tyrosine kinase signaling. *Mol Cancer Ther* **7**(10): 3129-3140.

Yarchoan M, Agarwal P, Villanueva A, Rao S, Dawson LA, Llovet JM, Finn RS, Groopman JD, El-Serag HB, Monga SP, Wang XW, Karin M, Schwartz RE, Tanabe KK, Roberts LR, Gunaratne PH, Tsung A, Brown KA, Lawrence TS, Salem R, Singal AG, Kim AK, Rabiee A, Resar L, Hoshida Y, He AR, Ghoshal K, Ryan PB, Jaffee EM, Guha C, Mishra L, Coleman CN and Ahmed MM (2019) Recent Developments and Therapeutic Strategies against Hepatocellular Carcinoma. *Cancer Res* **79**(17): 4326-4330.

Yoshikawa M, Morine Y, Ikemoto T, Imura S, Higashijima J, Iwahashi S, Saito YU, Takasu C, Yamada S, Ishikawa D, Teraoku H, Takata A, Yoshimoto T and Shimada M (2017) Elevated Preoperative Serum CEA Level Is Associated with Poor Prognosis in Patients with Hepatocellular Carcinoma Through the Epithelial-Mesenchymal Transition. *Anticancer Res* **37**(3): 1169-1175.

You A, Cao M, Guo Z, Zuo B, Gao J, Zhou H, Li H, Cui Y, Fang F, Zhang W, Song T, Li Q, Zhu X, Yin H, Sun H and Zhang T (2016) Metformin sensitizes sorafenib to inhibit postoperative recurrence and metastasis of hepatocellular carcinoma in orthotopic mouse models. *J Hematol Oncol* **9**: 20.

Younossi ZM, Golabi P, de Avila L, Minhui Paik J, Srishord M, Fukui N, Qiu Y, Burns L, Afendy A and Nader F (2019) The Global Epidemiology of NAFLD and NASH in Patients with type 2 diabetes: A Systematic Review and Meta-analysis. *J Hepatol*.

Zhang X, Harmsen WS, Mettler TA, Kim WR, Roberts RO, Therneau TM, Roberts LR and Chaiteerakij R (2014) Continuation of metformin use after a diagnosis of cirrhosis significantly improves survival of patients with diabetes. *Hepatology* **60**(6): 2008-2016.

- Zhang Y, Zha TZ, Hu BS, Jiang C, Ge ZJ, Zhang K and Tan YF (2013) High expression of ADAM8 correlates with poor prognosis in hepatocellular carcinoma. *Surgeon* **11**(2): 67-71.
- Zheng L, Yang W, Wu F, Wang C, Yu L, Tang L, Qiu B, Li Y, Guo L, Wu M, Feng G, Zou D and Wang H (2013) Prognostic significance of AMPK activation and therapeutic effects of metformin in hepatocellular carcinoma. *Clin Cancer Res* **19**(19): 5372-5380.
- Zhou YY, Zhu GQ, Liu T, Zheng JN, Cheng Z, Zou TT, Braddock M, Fu SW and Zheng MH (2016) Systematic Review with Network Meta-Analysis: Antidiabetic Medication and Risk of Hepatocellular Carcinoma. *Sci Rep* **6**: 33743.
- Zimmerman EI, Hu S, Roberts JL, Gibson AA, Orwick SJ, Li L, Sparreboom A and Baker SD (2013) Contribution of OATP1B1 and OATP1B3 to the disposition of sorafenib and sorafenib-glucuronide. *Clin Cancer Res* **19**(6): 1458-1466.

13. Footnotes

This work was supported by grants from Institut National de la Santé et de la Recherche Médicale (INSERM); Cancéropôle Ile de France; Institut National du Cancer (INCa-DGOS_5790); and the University of Sharjah (Competitive Grant no. 1701110321-P).

Reprint requests : Christèle Desbois-Mouthon, PhD
Centre de Recherche des Cordeliers
INSERM UMR_S1138
15 rue de l'école de médecine
75006 Paris
France
e-mail: christele.desbois-mouthon@inserm.fr

14. Figure legends

Figure 1. Effects of the concomitant and sequential combinations of metformin and sorafenib on tumor growth in a HCC xenograft model.

Six week-old athymic mice were inoculated s.c. with 2×10^6 PLC/PRF5 cells. Once tumor volumes reached 250 mm^3 , mice were treated by gavage with vehicles (control, n=19), sorafenib alone (15 mg/kg/day, n=10), metformin alone (50 mg/kg/day, n=14), metformin combined to sorafenib (concomitant schedule, n=8) or metformin followed 6 h later by sorafenib (sequential schedule, n=14). A, evolution of tumor volumes over the 15 days of treatment. *Inset*: representative photographs of tumors at sacrifice after concomitant or sequential treatment. B, tumor mass at sacrifice. *P* values were determined using Kruskal-Wallis test followed by Dunn's test as a post hoc test. *, $p < 0.05$; ***, $p < 0.001$; ###, $p < 0.001$.

Figure 2. Effects of the concomitant and sequential combinations of metformin and sorafenib on cell viability in human HCC cell lines.

A. PLC/PRF5, HepG2, Hep3B and Huh7 cell lines were seeded in 24-well plates (3×10^5 cells per well) and allowed to proliferate for 24 h in complete medium. Then cells were incubated for a further 72 h in the presence or not of metformin (1 mM), sorafenib (1 μM), metformin combined to sorafenib or metformin followed 6 h later by sorafenib. At the end of the treatment period, cell viability was measured using the MTT assay. Data are mean \pm SEM of three independent experiments performed in 8 determinations. *P* values were determined using Kruskal-Wallis test followed by Dunn's test as a post hoc test. *, $p < 0.05$; ***, $p < 0.001$.

B. Similar experiments were performed in PLC/PRF5 cells treated with different concentrations of metformin (0-0.5-1-2-3 mM) in combination with sorafenib (0-1-2 μ M). Data are mean of two independent experiments performed in 8 determinations.

Figure 3. Effects of the concomitant and sequential combinations of metformin and sorafenib on cell proliferation in human HCC cell lines.

PLC/PRF5 and Huh7 cell lines were seeded in 24-well plates (3×10^5 cells per well) and allowed to proliferate for 24 h in complete medium. Then cells were incubated for a further 72 h in the presence or not of metformin (1 mM), sorafenib (1 μ M), metformin combined to sorafenib or metformin followed 6 h later by sorafenib. At the end of the treatment period, cell proliferation was measured by cell counting (A) and staining DNA with 0.1% crystal violet (B). Data are mean of two independent experiments performed in 8 determinations.

Figure 4. Effects of metformin on the expression of efflux/influx transporters and sorafenib disposal in HCC cell lines.

(a, b) Total RNA was extracted from human hepatocytes in primary culture and HCC cell lines and quantitative measurements of transcripts coding for influx and efflux transporters were performed by real-time PCR.

(c, d) Uptake of [3 H]sorafenib over 10 min in Huh7 cells pre-treated during 6h in the presence of metformin (0-0.5-1-2-3-4 mM) at 37°C (c,d) or 4°C (d). Data are mean of two independent experiments performed in triplicates.

Figure 5. Effects of the concomitant and sequential combinations of metformin and sorafenib on the stimulation of AMPK phosphorylation in human HCC cell lines.

PLC/PRF5, HepG2, Hep3B and Huh7 cell lines were seeded in 24-well plates (3×10^5 cells per well) and allowed to proliferate for 24 h in complete medium. Then cells were incubated for a further 72 h in the presence or not of AICAR (0.5 mM), sorafenib (1 μ M), AICAR combined to sorafenib or AICAR followed 6 h later by sorafenib. (a) At the end of the treatment period, cell viability was measured using the MTT assay. Data are mean \pm SEM of three independent experiments performed in 8 determinations. *P* values were determined using Kruskal-Wallis test followed by Dunn's test as a post hoc test. *, *p* < 0.05; ***, *p* < 0.001. (b) Whole-cell lysates were analyzed by Western blotting for phosphorylated and total levels of AMPK. β -actin is used as a loading control. Blots are representative of two independent experiments.

Figure 6. Examples of signatures differentially modulated in xenografted tumors treated with concomitant and sequential metformin/sorafenib administration in comparison with control tumors.

A. Venn diagram showing the numbers of genes differentially expressed between the sequential and concomitant administration. 1035 genes were identified to be differentially expressed between control and concomitant treatments, 771 genes between control and sequential treatments, and 1051 genes between sequential and concomitant treatments. Among these differentially expressed genes, 193 genes were commonly altered by both types of treatments, while 842 genes were altered by the concomitant treatment only and 578 genes by the sequential treatment. B. Flowchart outlining the steps of the bioinformatics approach to identify differentially expressed

genes in concomitant and sequential treatments compared to controls. RNA samples were hybridized to Human Clariom™ S GeneChip. Following normalization using Signal Space Transformation-RMA (SST-RMA), differential expression was carried out using eBayes function and One-Way Anova statistical analysis. The analysis was carried out using Transcriptome Analysis Console software. The differentially expressed genes were then subjected to absolute GSEA searching through more than 10,000 different cellular pathways. C. Examples of signatures differentially modulated in xenografted tumors treated with concomitant and sequential metformin/sorafenib administration in comparison with control tumors. *Upper*, GSEA of GO_G_PROTEIN_COUPLED_RECEPTOR_ACTIVITY (GO:0007186) in HCC xenografts treated with concomitant combination of metformin and sorafenib in comparison with control group; *middle*, GSEA of GO_REGULATION_OF_PHOSPHORUS_METABOLIC_PROCESS (GO:0051174) in HCC xenografts treated with sequential combination of metformin followed by sorafenib in comparison with control group; *lower*, GSEA of BENPORATH_EED_TARGETS (M7617) in HCC xenografts treated with sequential combination of metformin followed by sorafenib in comparison with concomitant treatment.

15. Tables

Table 1. Plasma concentrations of metformin and sorafenib

	metformin (mg/L) (mean ± SD)		sorafenib (mg/L) (mean ± SD)	
	<i>2 h</i>	<i>4 h</i>	<i>2 h</i>	<i>6 h</i>
Monotherapy (n=3)	0.55 ± 0.18	0.30 ± 0.17	2.52 ± 1.03	0.66 ± 0.09
Concomitant (n=4)			2.32 ± 0.74	1.02 ± 0.39
sequential* (n=4)			2.99 ± 2.18	
sequential** (n=3)			3.46 ± 1.61	

* , metformin was administrated 2 h before sorafenib

** , metformin was administrated 4 h before sorafenib

Table 2. Relative tumor volumes and tumor growth inhibition rates

	RTV* (day 15)	%TGI** (day 15)
Control (n=19)	4.31	
Metformin (n=14)	3.80	11.72
Sorafenib (n=10)	2.49	42.31
Concomitant (n=8)	1.74	59.53
Sequential (n=14)	3.65	15.37

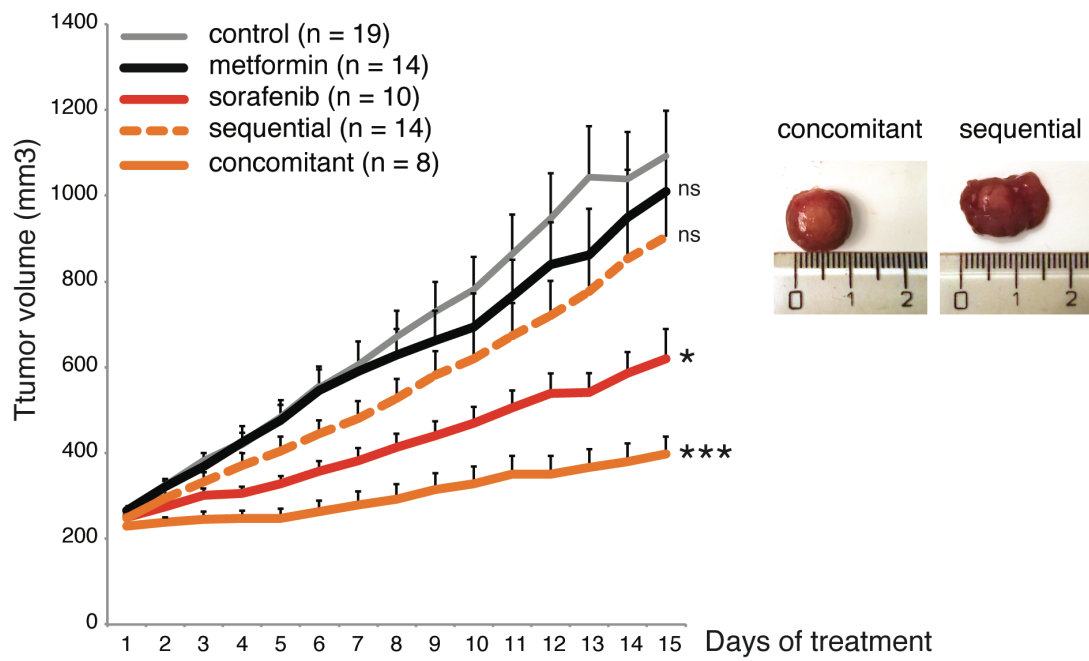
**Relative tumor volume (RTV) was calculated using the formula: TV_{d15}/TV_{d1} , where TV_{d15} and TV_{d1} are the mean tumor volumes at day 15 and day 1, respectively.*

***Tumor growth inhibition (TGI) rates were calculated using the formula : $(1 - TV_t/TV_c) * 100$, where TV_t and TV_c are the mean tumor volumes of treated and control groups, respectively.*

16. Figures

Figure 1

a



b

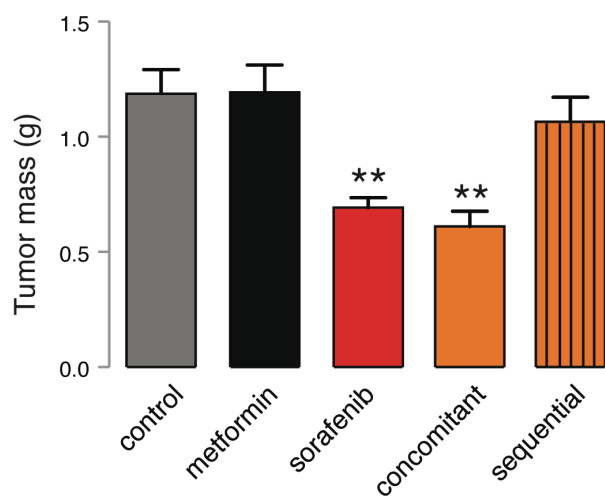


Figure 2

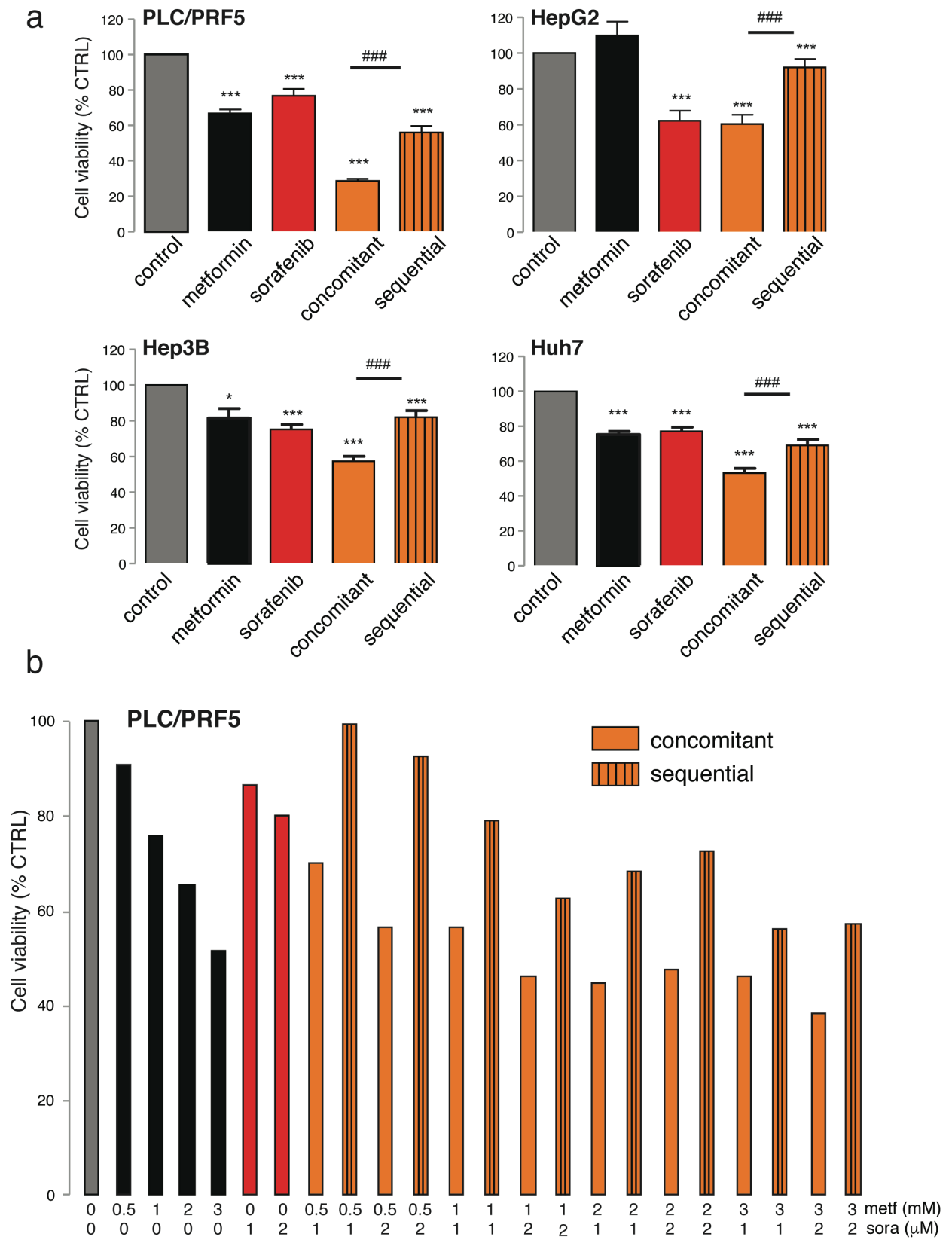
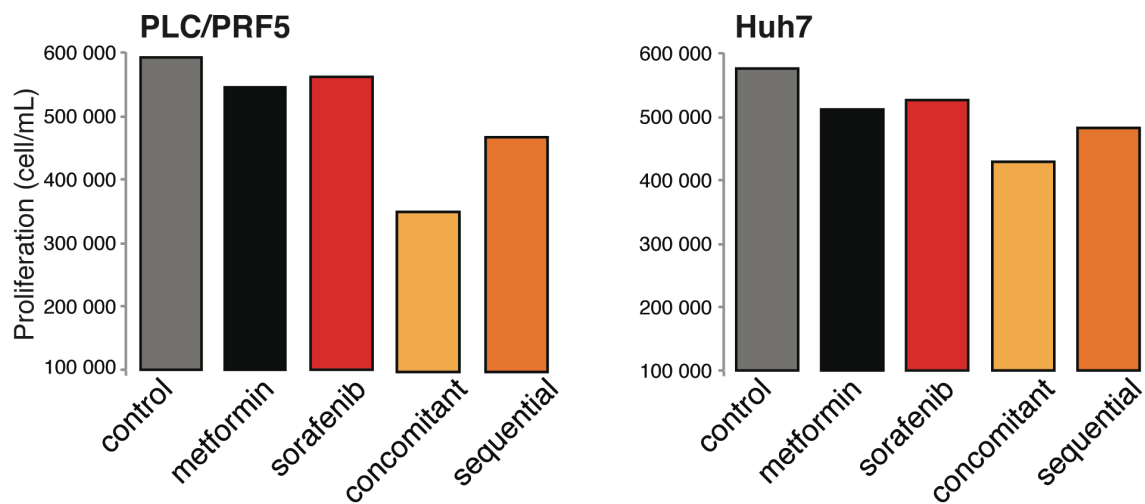


Figure 3

a



b

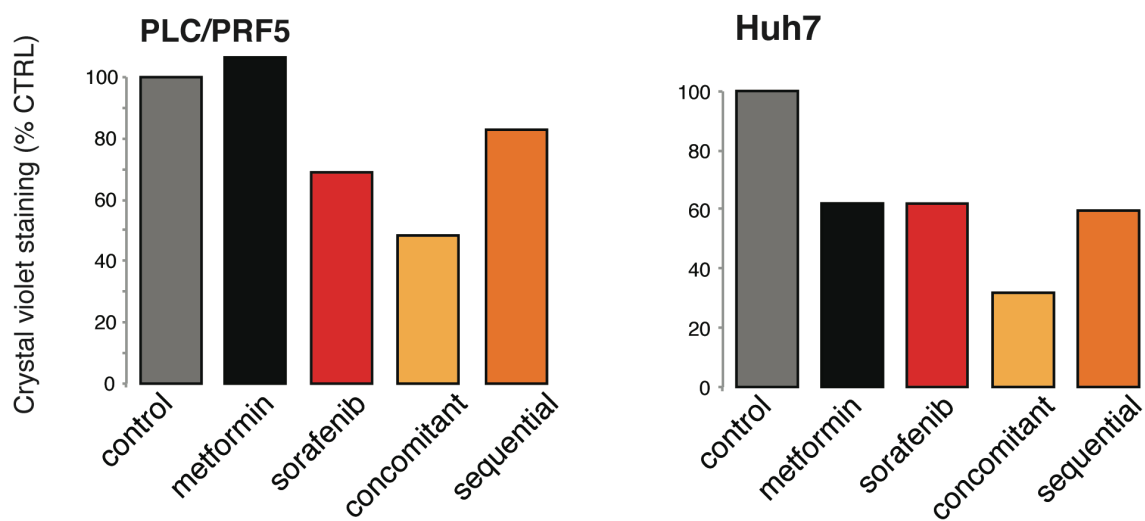


Figure 4

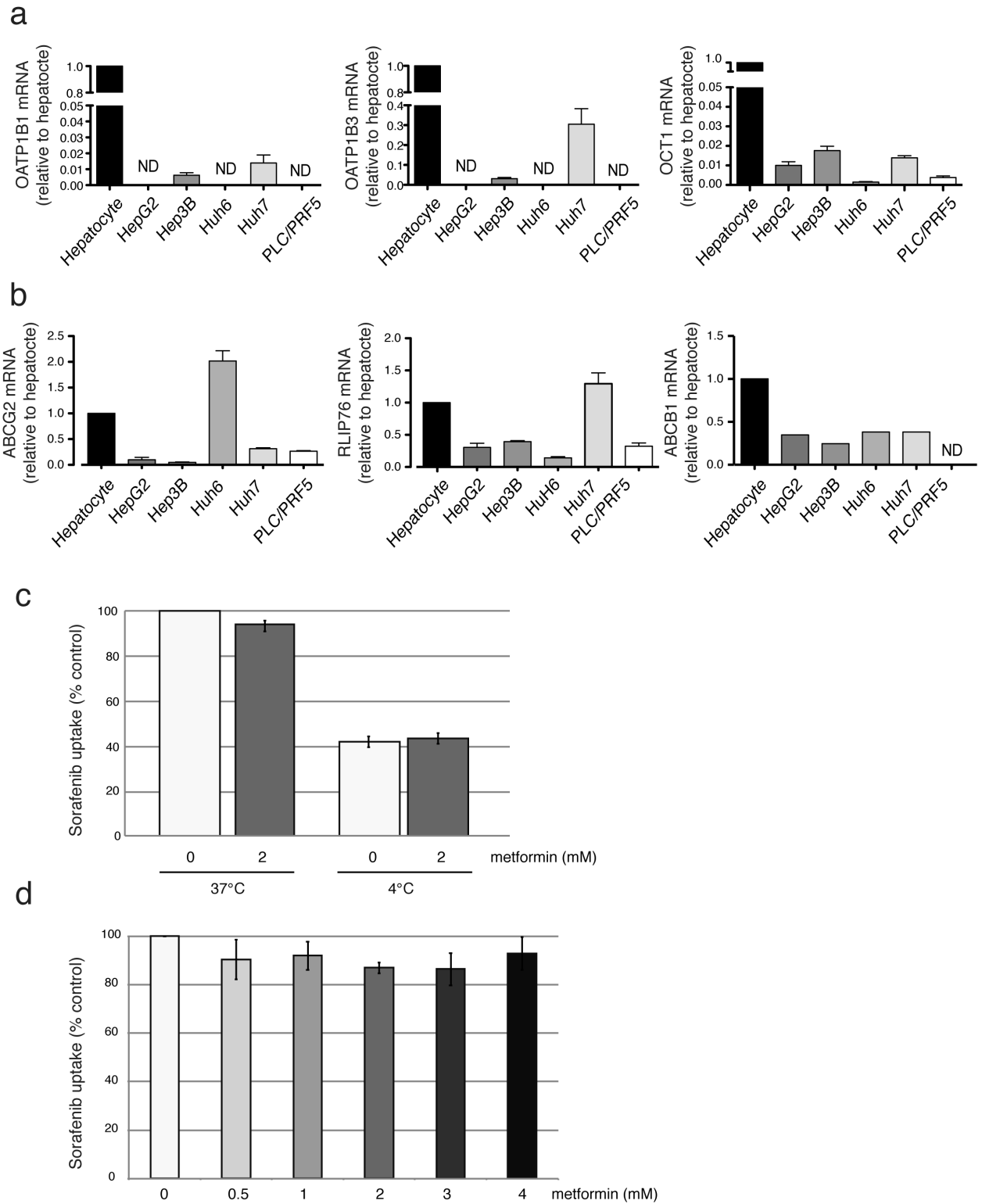
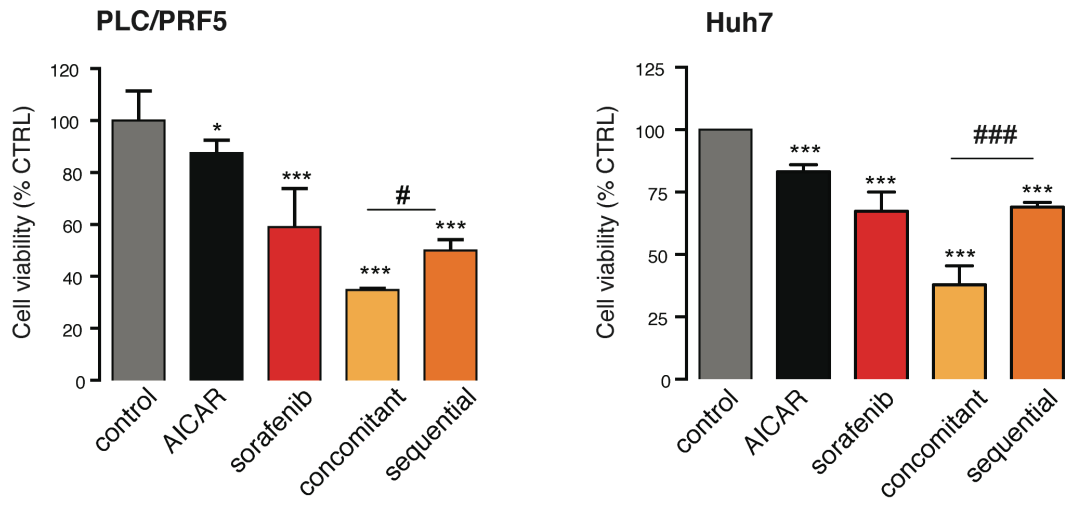


Figure 5

a



b

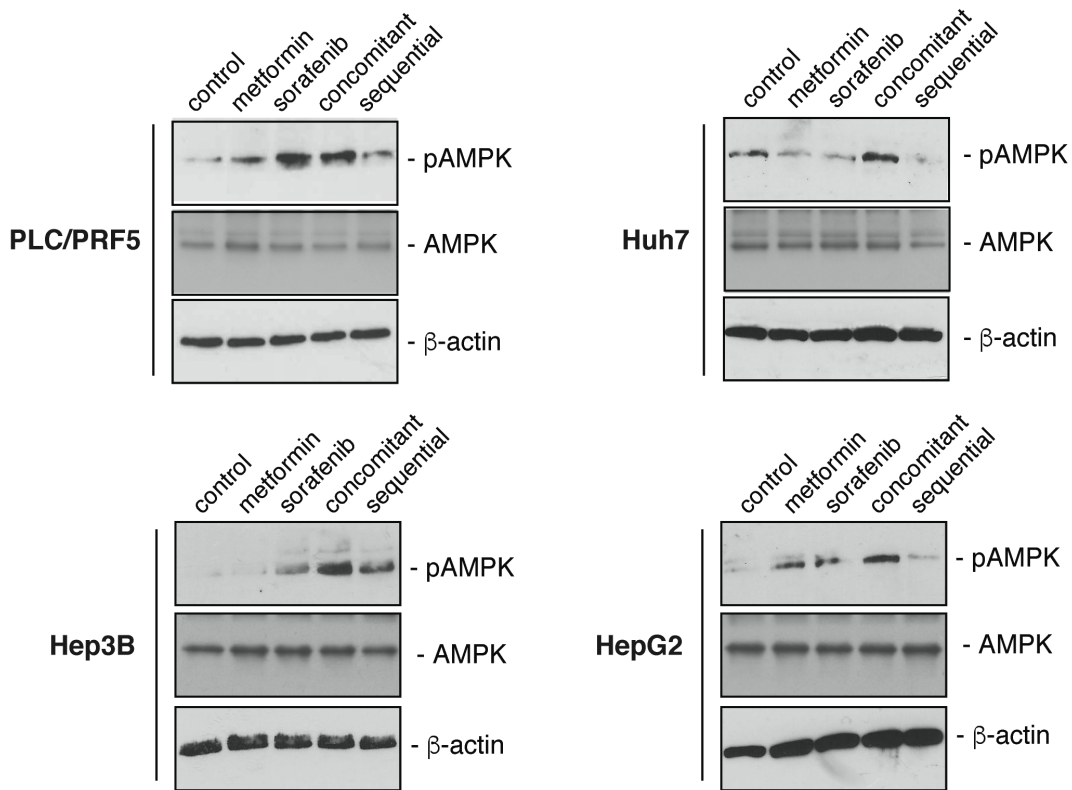


Figure 6

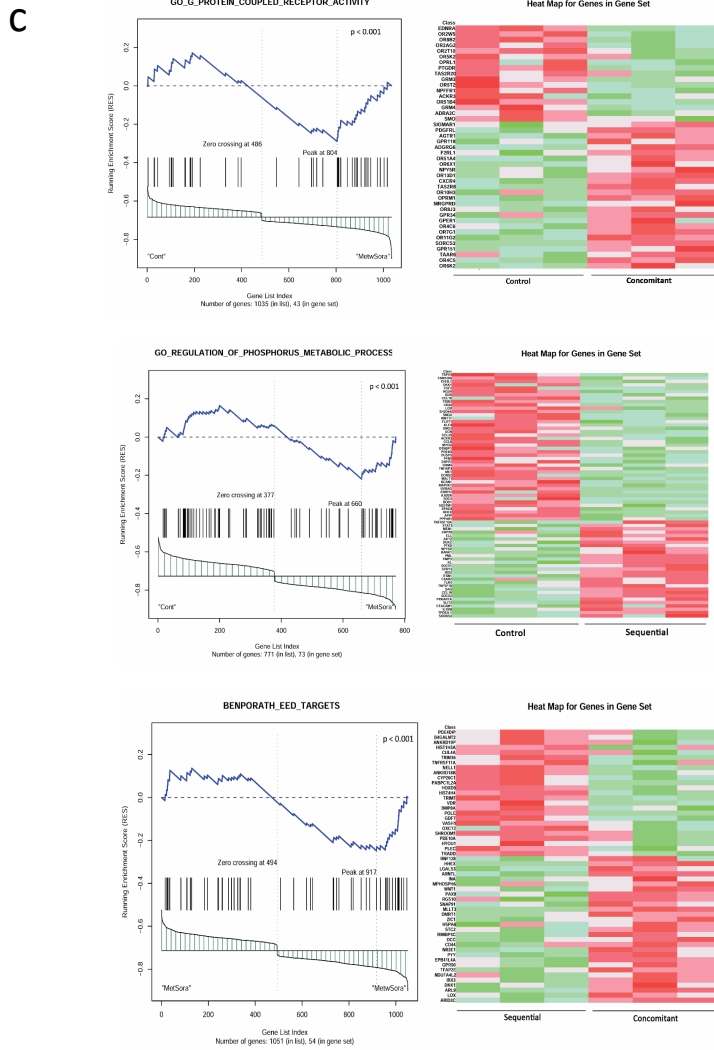
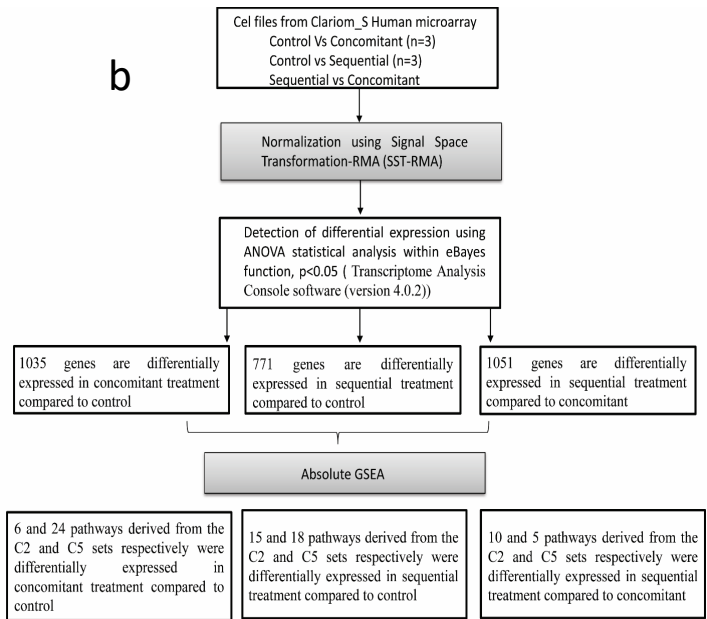
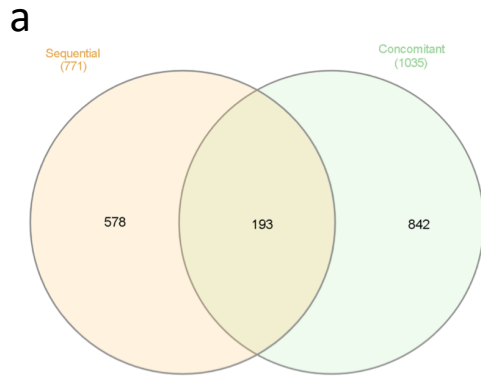
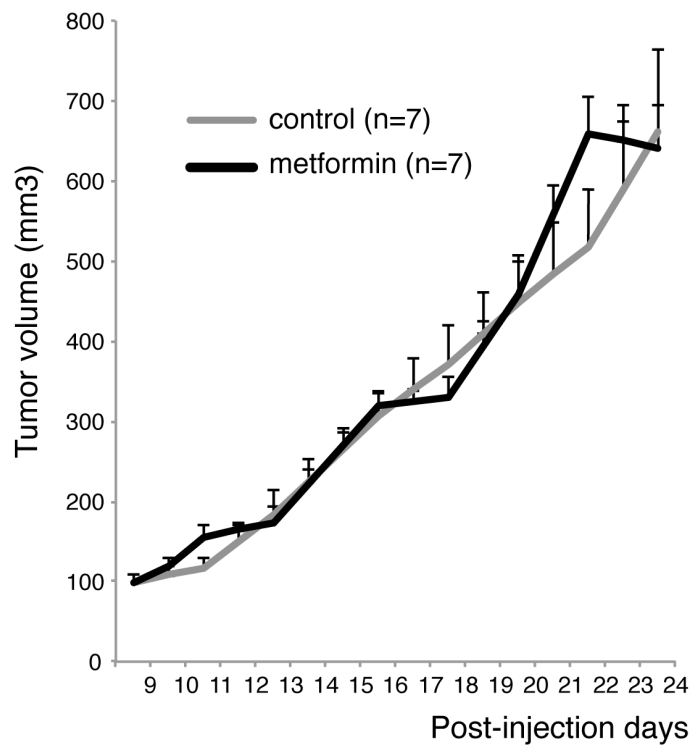
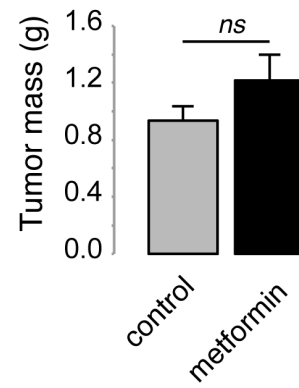


Figure S1

a



b



Supplemental figure legend

Figure S1. Effect of low dose metformin on tumor growth in a HCC xenograft model.

50 mg/kg/d metformin (n=7) and vehicle (n=7) were administrated to six week-old athymic mice four days before s.c. xenografts with 2×10^6 PLC/PRF5 cells and maintained during the next 15 days. A, evolution of tumor volumes over the 15 days of treatment. B, tumor mass at sacrifice.

Supplemental data

Table S1. Cellular pathways differentially expressed between control and concomitant treatments.

CONTROL versus CONCOMITANT TREATMENT						
c2						
GS	SIZE	ES	NES	Tag %	Gene %	Signal
REACTOME_G_ALPHA_S_SIGNALLING_EVENTS	21	0.53248	1.5112	0.952	0.448	0.536
REACTOME_OLFACTORY_SIGNALING_PATHWAY	16	0.56035	1.5103	1	0.448	0.56
KEGG_OLFACTORY_TRANSDUCTION	16	0.56035	1.4098	1	0.448	0.56
RAY_TUMORIGENESIS_BY_ERBB2_CDC25A_UP	15	0.52866	1.3987	0.667	0.271	0.493
REACTOME_PHOSPHOLIPID_METABOLISM	16	0.45114	1.3445	0.375	0.17	0.316
OSMAN_BLADDER_CANCER_DN	15	0.33939	1.2361	0.267	0.129	0.236
c5						
GO_SENSORY_PERCEPTION_OF_SMELL	18	0.56146	1.8089	1	0.448	0.561
GO_SENSORY_PERCEPTION_OF_CHEMICAL_STIMULUS	22	0.55972	1.805	1	0.452	0.56
GO_DETECTION_OF_STIMULUS_INVOLVED_IN_SENSORY_PERCEPTION	22	0.55972	1.7687	1	0.452	0.56
GO_OLFACTORY_RECEPTOR_ACTIVITY	17	0.5609	1.6738	1	0.448	0.561
GO_MONOCARBOXYLIC_ACID_METABOLIC_PROCESS	18	0.56383	1.5643	0.5	0.17	0.422
GO_DETECTION_OF_STIMULUS	30	0.50227	1.562	0.9	0.452	0.508
GO_LIPID_LOCALIZATION	16	0.70441	1.5321	0.625	0.136	0.548
GO_SENSORY_PERCEPTION	38	0.46803	1.513	0.842	0.452	0.479
GO_G_PROTEIN_COUPLED_RECEPTOR_ACTIVITY	43	0.43941	1.4741	0.791	0.448	0.455
GO_CYTOKINE_PRODUCTION	33	0.45672	1.455	0.424	0.168	0.365
GO_ORGANIC_ACID_METABOLIC_PROCESS	29	0.43233	1.4548	0.379	0.19	0.316
GO_TRANSMEMBRANE_SIGNALING_RECEPTOR_ACTIVITY	61	0.42633	1.4396	0.738	0.432	0.445
GO_MOLECULAR_TRANSDUCER_ACTIVITY	73	0.39116	1.4271	0.685	0.432	0.419
GO_ORGANONITROGEN_COMPOUND_CATABOLIC_PROCESS	50	0.32198	1.3997	0.28	0.19	0.238
GO_LIPID_METABOLIC_PROCESS	61	0.33109	1.3704	0.295	0.17	0.26
GO_MUSCLE_CONTRACTION	15	0.52138	1.3456	0.8	0.389	0.496
GO_REGULATION_OF_ION_TRANSPORT	31	0.35411	1.3031	0.613	0.421	0.366
GO_NERVOUS_SYSTEM_PROCESS	57	0.3831	1.2556	0.719	0.465	0.407
GO_POSITIVE_REGULATION_OF_CELL_ADHESION	22	0.46725	1.2534	0.773	0.409	0.467
GO_REGULATION_OF_CELL_ADHESION	38	0.41378	1.2423	0.658	0.409	0.404
GO_IMMUNE_SYSTEM_DEVELOPMENT	40	0.30727	1.1881	0.475	0.353	0.32
GO_PROTEIN_FOLDING	17	-0.43912	-1.5192	0.882	0.312	0.617
GO_REGULATION_OF_PROTEIN_STABILITY	17	-0.37789	-1.5042	0.765	0.257	0.578
GO_TRANSFERASE_COMPLEX	37	-0.23815	-1.235	0.838	0.504	0.431

Table S2. Cellular pathways differentially expressed between control and sequential treatments.

CONTROL Versus SEQUENTIAL TREATMENT						
c2						
GS	SIZE	ES	NES	Tag %	Gene %	Signal
NABA_MATRISOME_ASSOCIATED	39	0.4675	1.5113	0.615	0.305	0.451
RUIZ_TNC_TARGETS_UP	16	0.45342	1.5029	0.562	0.291	0.408
PEREZ_TP63_TARGETS	22	0.46613	1.482	0.5	0.227	0.398
BENPORATH_EED_TARGETS	43	0.36508	1.4746	0.674	0.447	0.395
YOSHIMURA_MAPK8_TARGETS_UP	52	0.36669	1.444	0.712	0.479	0.398
NABA_MATRISOME	53	0.47985	1.4232	0.623	0.305	0.465
REACTOME_SIGNALING_BY_RECEPTOR_TYROSINE_KINASES	21	0.43737	1.374	0.571	0.298	0.412
BLALOCK_ALZHEIMERS_DISEASE_DN	43	0.29838	1.3317	0.209	0.0934	0.201
CASORELLI_ACUTE_PROMYELOCYTIC_LEUKEMIA_DN	17	0.41419	1.2541	0.471	0.296	0.339
KINSEY_TARGETS_OF_EWSR1_FLII_FUSION_DN	22	0.46019	1.2428	0.545	0.254	0.419
HELLER_HDAC_TARGETS_SILENCED_BY_METHYLATION_DN	16	0.43541	1.1687	0.5	0.253	0.381
KRIGE_RESPONSE_TO_TOSEDOSTAT_24HR_DN	26	-0.40863	-1.8758	0.923	0.467	0.509
KRIGE_RESPONSE_TO_TOSEDOSTAT_6HR_DN	24	-0.38238	-1.7891	0.917	0.467	0.504
MILI_PSEUDOPODIA_HAPTOTAXIS_DN	29	-0.34525	-1.4426	0.862	0.435	0.507
SPIELMAN_LYMPHOBLAST_EUROPEAN_VS_ASIAN_DN	24	-0.3139	-1.3825	0.708	0.246	0.551
c5						
GO_POSITIVE_REGULATION_OF_LOCOMOTION	28	0.48911	1.505	0.536	0.22	0.433
GO_NEGATIVE_REGULATION_OF_MOLECULAR_FUNCTION	49	0.43343	1.486	0.571	0.326	0.412
GO_SENSORY_PERCEPTION	33	0.45354	1.4265	0.697	0.362	0.465
GO_DETECTION_OF_STIMULUS_INVOLVED_IN_SENSORY_PERCEPTION	17	0.51922	1.4184	0.765	0.333	0.521
GO_MOLECULAR_FUNCTION_REGULATOR	87	0.33807	1.4004	0.506	0.336	0.379
GO_MULTI_ORGANISM_REPRODUCTIVE_PROCESS	32	0.41586	1.3718	0.406	0.163	0.355
GO_IMPORT_INTO_CELL	31	0.39583	1.3694	0.548	0.296	0.402
GO_DEVELOPMENTAL_GROWTH	29	0.41256	1.3564	0.586	0.322	0.413
GO_MULTICELLULAR_ORGANISM_REPRODUCTION	30	0.37059	1.3486	0.367	0.163	0.319
GO_POSITIVE_REGULATION_OF_MAPK_CASCADE	26	0.42031	1.3077	0.538	0.272	0.405
GO_RECEPTOR_REGULATOR_ACTIVITY	24	0.40336	1.3066	0.5	0.223	0.401
GO_REGULATION_OF_PHOSPHORUS_METABOLIC_PROCESS	73	0.33339	1.2994	0.438	0.28	0.349
GO_POSITIVE_REGULATION_OF_PROTEIN_METABOLIC_PROCESS	64	0.29712	1.2922	0.516	0.39	0.343
GO_PROTEIN_DIMERIZATION_ACTIVITY	43	0.29309	1.2836	0.209	0.0921	0.201
GO_REGULATION_OF_DEVELOPMENTAL_GROWTH	16	0.39748	1.2468	0.438	0.202	0.356
GO_DETECTION_OF_STIMULUS	27	0.4875	1.2185	0.704	0.333	0.486
GO_ION_TRANSPORT	60	0.29029	1.2053	0.667	0.505	0.358
GO_REGULATION_OF_HORMONE_LEVELS	23	0.33721	1.1524	0.652	0.447	0.371

Table S3. Cellular pathways differentially expressed between sequential and concomitant treatments.

SEQUENTIAL Versus CONCURRENT TREATMENT						
c2						
GS	SIZE	ES	NES	Tag %	Gene %	Signal
REACTOME_ADAPTIVE_IMMUNE_SYSTEM	35	0.39285	1.5847	0.4	0.197	0.332
WANG_SMARCE1_TARGETS_DN	20	0.43017	1.4106	0.35	0.127	0.311
REACTOME_SIGNALING_BY_GPCR	52	0.39552	1.4082	0.654	0.384	0.423
BENPORATH_ES_WITH_H3K27ME3	58	0.35724	1.3813	0.586	0.375	0.388
BENPORATH_EED_TARGETS	54	0.36791	1.38	0.481	0.266	0.372
REACTOME_INTERFERON_SIGNALING	18	0.52672	1.3793	0.722	0.283	0.527
MARTENS_TRETINOIN_RESPONSE_DN	45	0.34329	1.3265	0.489	0.313	0.351
REACTOME_GPCR_LIGAND_BINDING	21	0.44477	1.2749	0.714	0.384	0.449
ZHOU_INFLAMMATORY_RESPONSE_LIVE_DN	16	0.44659	1.2659	0.562	0.253	0.427
RICKMAN_METASTASIS_UP	15	0.30025	1.2378	0.6	0.451	0.334
c5						
GO_HEART_DEVELOPMENT	28	0.4566	1.608	0.429	0.168	0.366
GO_SIDE_OF_MEMBRANE	24	0.45037	1.4105	0.833	0.441	0.477
GO_EXTERNAL_SIDE_OF_PLASMA_MEMBRANE	18	0.49006	1.3623	0.889	0.441	0.506
GO_G_PROTEIN_COUPLED_RECEPTOR_ACTIVITY	27	0.41388	1.3031	0.741	0.432	0.432
GO_CELLULAR_RESPONSE_TO_OXIDATIVE_STRESS	16	-0.45287	-1.7236	0.938	0.462	0.512

Table S4. Genes differentially expressed in more than three different pathways and considered of significance for the drug mechanism of action

Concomitant Treatment
C2 (Upregulated genes)
OR4C6
C2 (Downregulated genes)
OR2AG2
C5 (Upregulated genes)
CEACAM1; OR10H3; OR11G2; OR13D1; OR4C5; OR4C6; OR51A4; OR6K2; OR6X1; OR7G1; OR8J3; SCN1A; ADAM8; ARG1; ASIC3; PRNP; TAS2R8; GPER1; IL7; SPX; TRPM5; VNN1
C5 (Downregulated genes)
OR2AG2; OR2T10; OR2W5; OR51B4; OR5K2; OR5T2; OR8B2; BBS4; TAS2R20; ANK3; KAT2A; PIEZO2; PRKD2
Sequential Treatment
C2 (Upregulated genes)
CTSD; IL1RN ; TMEM97
C2 (Downregulated genes)
SFPQ; AKAP2; COL1A1; COL1A2; LOX; SOX4
C5 (Upregulated genes)
PRKAR1A; SLIT2; STAT3; STAT5B; ILR1N; IRS2; AKT2; CCL16; CEACAM1; KL; NPY5R; SEMA6B; SEMA6C; TLR4; TNFSF18; APOA5; CGA; DKK3; ERP29; KALRN; LIMK1; MEN1; PKD2L1; PML; SAG; SOCS1; SOCS2; TIMP3; TPD52L1; TRPA1
C5 (Downregulated genes)
FGF2; UCN; CCL8; DKK1; RGS4; CCL20; TRPV4; ACKR3; BIRC3; CCL18; GIP; PRL; WNT11; AJUBA; BEST1; CD44; CUBN; DUSP5; ENPP2; FLOT1; HMOX1; KDR; KLF4; MAP2K1; OPRL1; PER2; PIP; PMCH; SOX4; SPAG9; TRIB2
Sequential vs Concomitant Treatment
C2 (Upregulated genes in sequential compared to concomitant)
PDE4DIP
C2 (Downregulated genes in sequential compared to concomitant)
PYY; WNT1
C5 (Upregulated genes in sequential compared to concomitant)
-
C5 (Downregulated genes in sequential compared to concomitant)
-